OT REPORT 76-107

ANOMALOUS PROPAGATION AND INTERFERENCE FIELDS

OT

U.S. DEPARTMENT OF COMMERCE/Office of Telecommunications

OT REPORT 76-107

ANOMALOUS PROPAGATION AND INTERFERENCE FIELDS

H.T. DOUGHERTY
B.A. HART

U.S. DEPARTMENT OF COMMERCE
Elliot L. Richardson, Secretary

Betsy Ancker-Johnson, Ph. D.
Assistant Secretary for Science and Technology

OFFICE OF TELECOMMUNICATIONS
John M. Richardson, Director

December 1976

UNITED STATES DEPARTMENT OF COMMERCE
OFFICE OF TELECOMMUNICATIONS
STATEMENT OF MISSION

The mission of the Office of Telecommunications in the Department of Commerce is to assist the Department in fostering, serving, and promoting the nation's economic development and technological advancement by improving man's comprehension of telecommunication science and by assuring effective use and growth of the nation's telecommunication resources.

In carrying out this mission, the Office

- Conducts research needed in the evaluation and development of policy as required by the Department of Commerce
- Assists other government agencies in the use of telecommunications
- Conducts research, engineering, and analysis in the general field of telecommunication science to meet government needs
- Acquires, analyzes, synthesizes, and disseminates information for the efficient use of the nation's telecommunication resources.
- Performs analysis, engineering, and related administrative functions responsive to the needs of the Director of the Office of Telecommunications Policy, Executive Office of the President, in the performance of his responsibilities for the management of the radio spectrum
- Conducts research needed in the evaluation and development of telecommunication policy as required by the Office of Telecommunications Policy, pursuant to Executive Order 11556

USCOMM - ERL

TABLE OF CONTENTS

		Page
LIST OF FIGURES		iv
ABSTRACT		1
1.	INTRODUCTION	2
2.	PROPAGATION VIA HIGH ELEVATED LAYERS	5
	2.1 Enhanced Field Characteristics	9
	2.2 Occurrence of Elevated Layers	11
	2.3 Tropospheric Versus Sporadic-E Enhanced Fields	19
3.	PROPAGATION VIA STRONG SURFACE DUCTS	20
	3.1 Sea-Surface Ducting	21
	3.2 Superrefractive Advection Layers	23
	3.3 Evaporation Layers	25
	3.4 Subrefractive Advection Layers	30
	3.5 Overwater Prediction Charts	31
4.	THE ANOMALOUS FIELDS	41
	4.1 Duct Geometry	43
	4.2 Approximations For Interference Estimates	49
	4.3 Occurrence	52
5.	CONCLUSION	55
6.	REFERENCES	57

LIST OF FIGURES

Figure		Page
1.	Geometry for the enhanced-field mode of propagation via an elevated layer.	6
2.	Transhorizon 185.75 MHz signals recorded at GBH, Colorado.	10
3.	Percent occurrence contours for the Atlantic trade wind inversion in February.	12
4.	Contours of the mean refractivity gradient (in N units/km) for the Atlantic trade wind inversion in February.	13
5.	Contours of the mean layer thickness (in meters) for the Atlantic trade wind inversion in February.	14
6.	Contours of the mean layer base height (in kilometers) for the Atlantic trade wind inversion in February.	15
7.	Areas of the world's oceans where conditions are favorable for the formation of elevated layers.	16
8.	Mean heights (in meters) and percent occurrences (>40%) for elevated layers with gradients ≤-157.	18
9.	Identification of the propagation mode for locations of a transmitter above the duct (top drawing) and within the duct (bottom drawing).	22
10.	Surface currents of the oceans in February-March.	24
11.	Surface temperatures of the oceans in February.	26
12.	Surface temperatures of the oceans in August.	28
13.	Areas of the world where evaporation exceeds precipitation.	29
14.	Regions for which charts are available primarily of advective layers and primarily of evaporative layers.	32
15.	Percent expectancy of extended coverage, S-band radar, Southeast Asia, January.	34

LIST OF FIGURES (Continued)

Figure		Page
16a.	Percent of time trapping frequency <300 Hz, August.	35
16b.	Percent of time trapping frequency <3000 Hz, November.	35
17a.	Refractivity lapse rates (N/km) not exceeded 5 percent of time for 100 m layer, August.	36
17b.	Refractivity lapse rates (N/km) not exceeded 2 percent of time for 100 m layer, August.	36
18a.	Percent of time gradient ≤-100 (N/km), August.	38
18b.	Percent of superrefractive layers thicker than 100 m, August.	38
19.	February and August median values of 100 m refractivity gradient.	39
20.	Observed gradients at Bangui, Central Africian Republic.	40
21.	Diurnal variability in surface refractivity gradients.	42
22.	Elevated-layer and surface-layer parameters for ducting conditions.	44
23	Ray-theory representations of elevated-duct propagation.	48

ANOMALOUS PROPAGATION AND INTERFERENCE FIELDS

H. T. Dougherty[+] and B. A. Hart[*]

This report presents some estimates of the enhanced fields deduced from the presently available theory and observational data. The fields of interest are the enhanced fields that are encountered in the presence of the stratified atmosphere, the ducting conditions associated with supercritical refractivity gradients both near the surface and aloft.

As a basis for estimating the likelihood of occurrence of these supportive conditions, the available information is surveyed. It is suggested that the access to computers and the availability of historical radiosonde data be exploited and the pertinent characteristics of elevated layers and their associated ducts be mapped on a worldwide basis to meet the interference prediction requirements of regulatory agencies.

1. INTRODUCTION

As the operation of telecommunication systems has been implemented for higher and higher transmission frequencies, the earth's atmosphere has played an increasingly significant role. For example, the atmospheric bending of a radio wave's path of propagation (refraction) is determined by the atmosphere's refractivity gradient. This is often expressed in terms of an equivalent earth's radius factor, $k = r/r_o$, $r_o \approx 6370$ km, that varies from approximately 1.0 at about 0.1 MHz to approximately 4/3 for 100 MHz and higher frequencies [Rotheram, 1970]. At 30 MHz and higher frequencies,

---

[+]The author is with the Institute for Telecommunication Sciences, Office of Telecommunications, U.S. Department of Commerce, Boulder, Colorado 80302.

[*]The author is with the Policy Research Division, Office of Telecommunications, U.S. Department of Commerce, Boulder, Colorado 80302.

this median refraction is better described in terms of the refractivity structure, the change of refractivity with height above the earth's surface. Then, the seasonal and geographical variation of this refractivity structure may be described in terms of a standard median refractivity model [Bean et al., 1966; Bean and Dutton, 1968; CCIR, 1974a].

For such standard conditions, the applicable mode of radio wave propagation is identifiable from the path parameters, and its characteristics are predictable by classical methods that approximate the atmosphere as a homogeneous medium. For some portion of the time at most locations, the refractivity structure near the surface and at elevated levels will depart markedly from the model structure. Nevertheless, for 30 MHz and lower frequencies, even this stratified atmosphere is no problem because the vertical dimensions of the associated refractivity structures are very small in terms of wavelength; the atmosphere averages to an exponential structure whose effect is readily approximated by modification of the standard prediction methods [Rotheram, 1970; Gerks, 1971]. However, as the frequency of interest is extended to VHF and higher, the effects of these non-standard conditions become increasingly significant. The resulting modes of propagation are anomalous. Anomalous (or non-standard) refers to those conditions for which received radio fields are markedly stronger or weaker than would be expected for a standard atmosphere. There may be either a serious degradation or a marked improvement in the signal's level, fading rate, or fade duration. For most paths, either effect is possible and is determined by both the path geometry and the spatial distribution of the marked departures of the refractivity structure from the model.

The anomalous degradation of the received signal (fading) has been the subject of many theoretical and experimental investigations of line-of-sight propagation paths. These are

well-documented [Beckman and Spizzichino, 1963; Dougherty, 1964], and the results have been suveyed and categorized [Dougherty, 1968; White, 1968]. This signal degradation (fading) due to anomalous propagation is serious because it directly impairs system performance; it is an intrasystem problem for which remedies are applied (either in anticipation or after-the-fact) so as to assure that the required system reliability is achieved.

On the other hand, the anomalous improvement of the received signal (an enhanced field) is primarily of interest because the more volatile problem of intersystem interference can result, particularly for beyond-line-of-sight paths. These paths, generally referred to as transhorizon paths, normally involve propagation via the troposcatter or the diffraction modes. Since they pose the threat of interference to or from other systems, the occurrence of the enhanced fields take on increased importance. It is these anomalous fields (these uncommon, enhanced fields) which largely determine coordination distances required by the (national and international) regulatory agencies (CCIR, 1974b). Somewhat optimistic estimates of unusually strong fields and the liklihood of their occurrence are required in order to avoid their serious impact as intersystem interference. Anticipation of this latter problem is one of continuing urgency for our national regulatory agencies, particularly in view of the World General Administrative Radio Conference of the International Telecommunications Union (WGARC-79) scheduled for 1979.

It is the longer transhorizon paths (for which the standard mode of propagation is troposcatter) that exhibit the most dramatic enhancement of fields due to anomalous propagation. The standard, attenuated, rapidly fluctuating troposcatter signal may be replaced by a strong, slowly varying signal. These enhanced fields occur in the presence

of an elevated, strong, atmospheric layer. Although their investigation covers three decades, such enhanced fields have not been studied as extensively as have the degraded (fading) line-of-sight fields and they are not as well understood in a quantitative sense. Section 2 of this report summarizes the present state of our knowledge of these enhanced fields that are propagated by elevated layers.

For short transhorizon paths (for which the standard mode of propagation is diffraction), the enhanced fields are on the order of the free-space field. Their occurrence, ducting, is almost always associated with the presence of strong refractivity gradients at or near the surface; these are more common on maritime or over-water paths. Such enhanced fields have also been the subject of investigation for almost three decades. These ducted fields are better understood, in a quantitative sense, than are the enhanced fields associated with elevated layers, but they are still less well understood than the degraded line-of-sight fields. Section 3 of this report summarizes the present state of our knowledge of enhanced fields that are associated with strong layers at or near the surface, (ducted fields).

Section 4 of this report summarizes the problem of estimating the field strengths of these anomalous fields and their impact for interference-avoidance purposes. Section 5 contains the conclusions and recommendations of this report. Section 6 provides the references of this report, a virtual roll-call of nations.

2. PROPAGATION VIA HIGH ELEVATED LAYERS

Many investigators have reported unusually strong signals (at or approaching free-space levels) received over transhorizon paths. Further, they have associated their observations with weather processes known to produce high, elevated, atmospheric layers (on the order of a kilometer or so above the surface) [Day and Trolese, 1950; Hirao et al., 1952; Arrola, 1957; Ringwalt et al., 1958; Ringwalt and MacDonald, 1961; Misme, 1960; Ament et al., 1962; Vergara et al., 1962; Gough, 1962; Guinard et al., 1964; Lane and Sollum, 1965; Lane and Owolabi, 1969; Owolabi and Lane, 1973]. A strong correlation has been found between received-signal strength and the occurrence of elevated layers at elevations below the base of the troposcatter common volume. This has led to an empirical dependence of received signal strength upon: the magnitude of the layer refractivity gradient, the elevation of the layer base, and/or the angle of incidence of the signal ray path at the layer base. Multiple reflection from elevated layers has been proposed as the significant mechanism in transhorizon propagation [Saxton, 1951; Ament, 1959; Hall, 1968a, 1968b; Paltridge, 1970]. Empirical studies have deduced similar expressions for the coupling efficiency and propagation loss [Skillman, 1969; Misme, 1973; 1974; CCIR, 1974b].

Although the mechanism (reflection, scatter, etc.) by which the incident radio energy is redirected at the atmospheric layer is still uncertain (in a quantitative sense), propagation via elevated layers may be said to have an experimental and theoretical basis. The situation is illustrated by the schematic representation of the attached figure 1. There, the dashed lines indicate the radio ray paths whose intersection defines the common volume base and scattering angle for the standard troposcatter propagation path. In the presence of the indicated elevated atmospheric layer, the

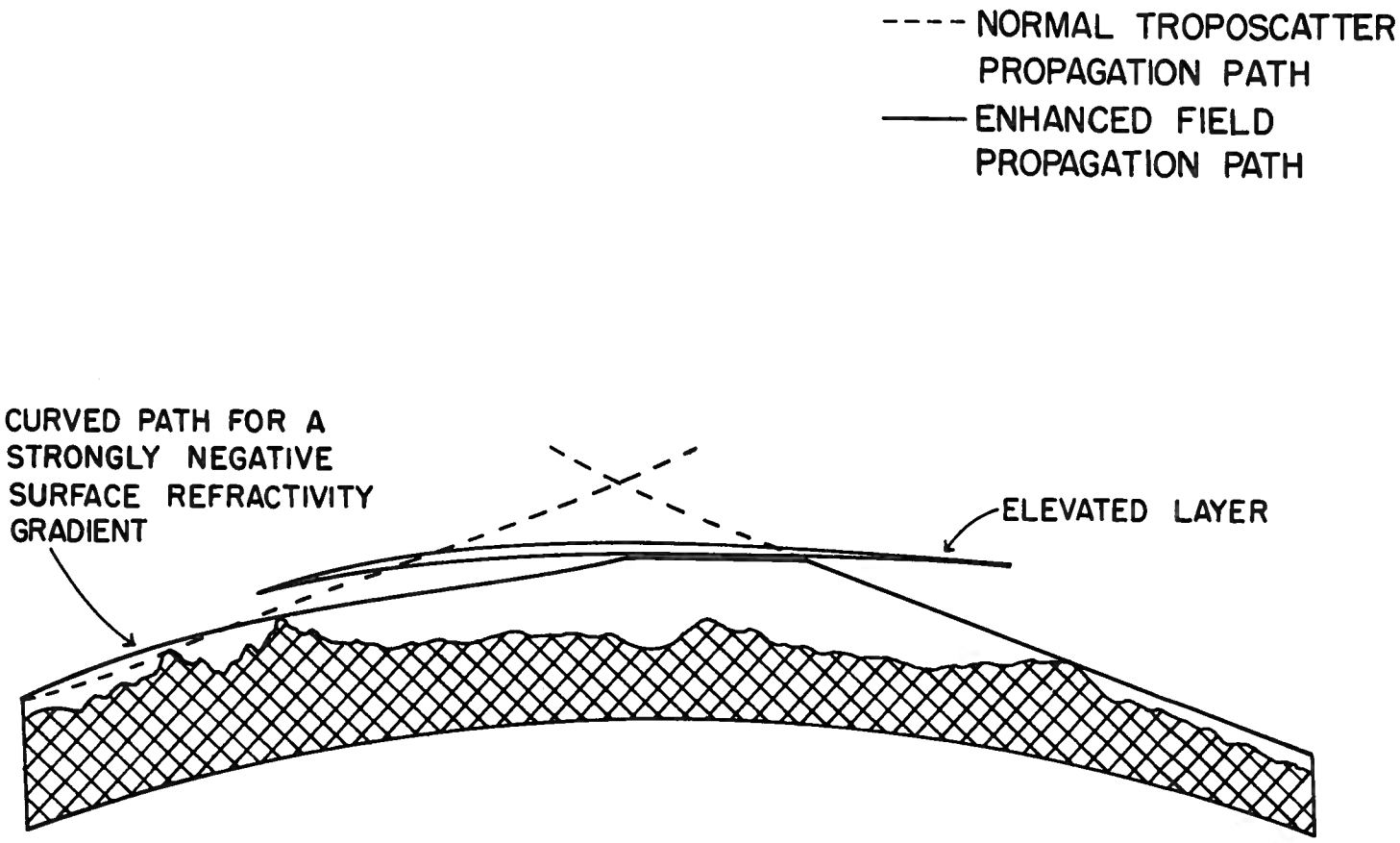

Figure 1. Geometry for the enhanced-field mode of propagation via an elevated layer.

intersection of the dashed lines with the layer base will produce a redirection of radio energy generally parallel to the layer; both the reflection from local irregularities of the layer base and also the scattering-at-and-propagation-along the layer base have been proposed as possibilities. In either case, this redirection of energy increases in efficiency as the grazing angle (between the radio ray path and the layer base) approaches zero. Thus, a reduction in layer height would decrease grazing angle and increase the energy-coupling efficiency. Similarly, the increased ray-bending (refraction) that would occur for a more strongly negative refractivity gradient near the surface (between a terminal and its horizon) would also decrease the grazing angle and increase the coupling efficiency at the layer. A lack of layer continuity between the points for which the solid-line ray path of figure 1 parallels the layer could introduce additional coupling losses (from layer segment-to-layer segment) for guided propagation along the layer base, but may not for propagation by multiple reflection from the layer.

There are a variety of formulas for reflection from an atmospheric layer, depending upon the assumed variation of the refractive index through the layer (Brekhovskikh, 1960; duCastel et al., 1960; Yamada, 1961; Wait, 1962; Wait and Jackson, 1964; Thayer, 1970). For example, the coefficient of reflection from a planar discontinuity, Δm, in the modified refractive index is given by

$$|R|_o = \frac{|\Delta m|}{2 \sin^2\theta} , \quad \theta>0 . \tag{1a}$$

Here, the grazing-angle-of-incidence θ at the discontinuity (H meters above and d kilometers from the radio terminal) is given by

$$\theta \approx \frac{H}{d} + dG \tag{1b}$$

in milliradians. The G is the modified refractivity gradient (in M units/km) below the discontinuity, determined from the refractivity gradient (g in N units/km) by

$$G = g + 157 = \left[\frac{\Delta n}{\Delta h} + \frac{1}{r_o}\right] 10^6 \ . \tag{1c}$$

This is described further in Section 4.

For an atmospheric layer with a linear decrease in modified refractivity Δm across a layer thickness of h in the same units as the transmission wavelength λ, the internal reflection coefficient is given by the product (Wait, 1962; 1964)

$$|R| = |R|_o \left|\frac{\sin X}{X}\right| \ , \quad X = 2\pi \frac{h}{\lambda} \sin\theta \ . \tag{2a}$$

An optimistic estimate of the internal reflection coefficient for elevated layers may be obtained from the envelope of (2a),

$$|\tilde{R}| = \frac{\Delta m \ \lambda}{4\pi h \ \sin^3\theta} \ . \tag{2b}$$

This is twice the value that would be obtained if the gradient $\Delta m/h$ were maintained over an infinite depth (Wait, 1964).

Each of the foregoing expressions are optimistic in the sense that they assume the elevated atmospheric layer (or discontinuity in refractivity) is smooth, planar, and of unlimited horizontal extent. Factors are available to modify these reflection coefficients for the effects of roughness (in terms of the standard deviation of the surface about its mean) and of limited horizontal extent (when the horizontal

extent is expressed in terms of Fresnel Zones) [Beckmann and Spizzichino, 1963; Dougherty, 1968].

For short transhorizon paths, the propagation via layer reflection can involve Saxton's four ray paths [1951]. He identified propagation by four paths, each involving one layer reflection. Further, one of the paths involved no other reflections, two paths each also involved a single reflection from the foreground of one antenna, the fourth path involved reflection from both foregrounds. Hall [1968a and 1968b] proposed two reflections from the elevated layers as providing the direct path; however, this appears similar to one of Wait's [1962] earth-detached modes of propagation through an elevated duct.

2.1 Enhanced Field Characteristics

The enhanced fields observed on normally troposcatter paths have been reported for a wide range of transmission frequencies from VHF to EHF, for a variety of path lengths from 100 to more than 1000 km, and at levels up to 40 dB <u>above</u> the long-term troposcatter median level. A recent experimental investigation in Colorado of a 376 and a 633 km overland path at 185.75 MHz (from KOMC, Kansas, and KHQL, Nebraska, respectively), provided a quantitative description of the observed enhanced fields [Dougherty et al., 1970]. Over a 13 month period, the enhanced fields occurred on the 376 km path with hourly median levels of 15 dB or more above the long-term hourly median during 6% of the morning hours (0600 to 1200 hours local time) from mid-May to mid-August. The enhanced fields were observed about half as often on the 633 km path. The highest observed hourly median was 48 dB (above the long-term hourly median) on the 633 km path and 44 dB on the 376 km path. This latter value is only 21 dB below the theoretical free-space level of the 376 km path.

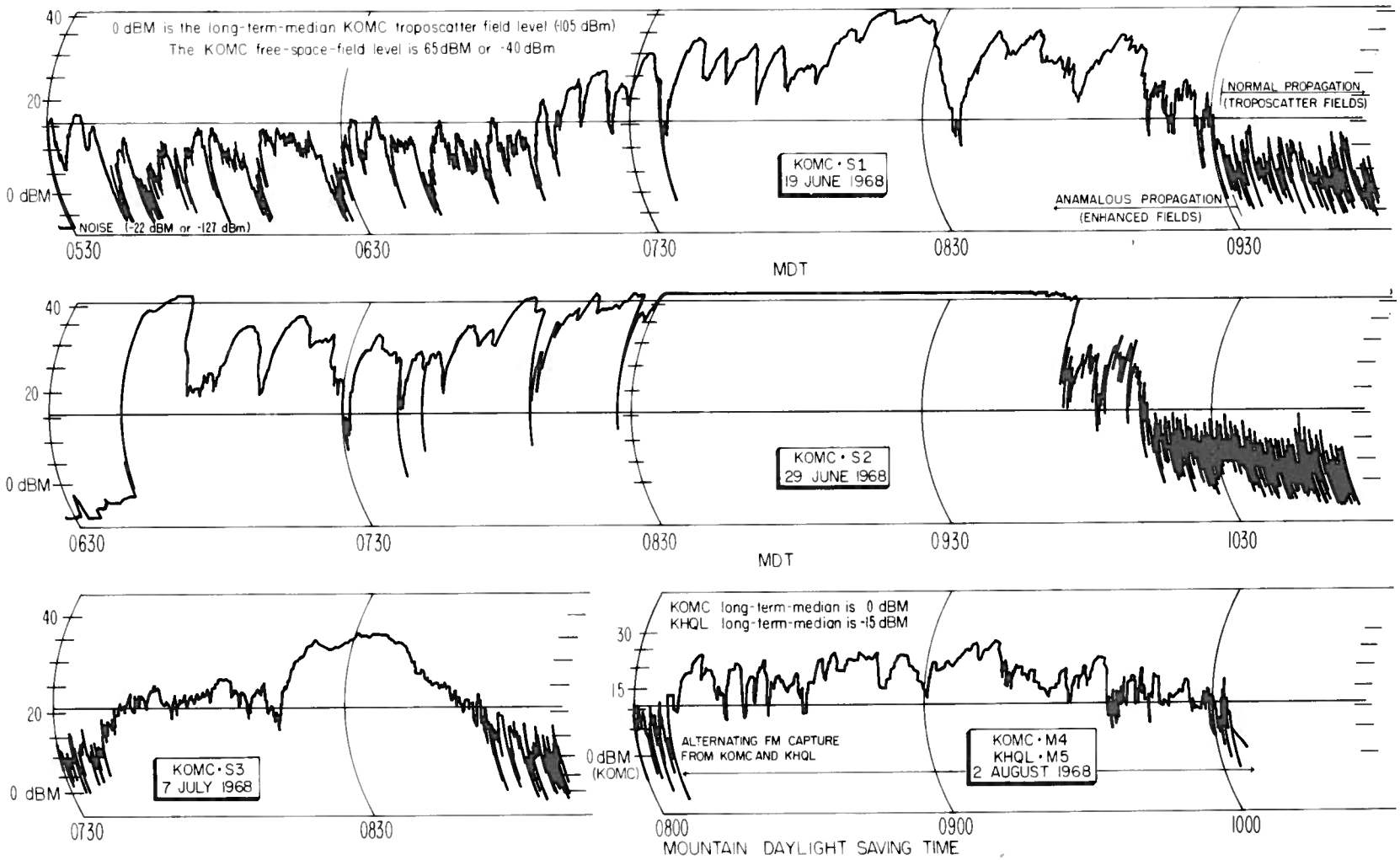

Figure 2. Transhorizon 185.75 MHz signals recorded at GBH, Colorado [Dougherty et al., 1970].

The strongly-enhanced-field events were marked by slowly varying signals with occasional deep fades of short duration, and although they occasionally exhibited fading characteristics which could be described in terms of the parameters usually employed for troposcatter fields (moderately enhanced fields), their fading rates and durations differed from those of troposcatter by one or more orders of magnitude. The strongly enhanced fields are illustrated by events S1, S2, and S3 in figure 2; the moderately enhanced fields are illustrated by events M4 and M5 [Dougherty et al., 1970]. On one occasion, the signal exceeded 40 dB above the long-term hourly median (24 dB below the free-space level) for 91 minutes.

2.2 Occurrence of Elevated Layers

These enhanced fields occurred in the presence of atmospheric subsidence that produced elevated layers generally consisting of dry warm air overlying cool moist air. For 80% of these enhanced field events, strong surface refractivity gradients were observed. Although they were more common for "summer mornings", two events occurred in each of the months of January and February and one event occurred between 2000 and 2400 hours local time in July. One would therefore expect that these tropospheric layers that are conducive to high fields will occur over large land masses generally because of subsidence effects. Advection can also produce these same conditions, particularly in coastal regions, although more frequently over the water than over the land. Subsidence is also the mechanism that produces the semi-permanent trade wind elevated layers, roughly 5°N to 30°N and 5°S to 30°S, over the oceans. An example of these elevated layers are illustrated by figures 3, 4, 5, and 6 [Doughety et al., 1967]. Published information also suggests similar (though less common) elevated layers over

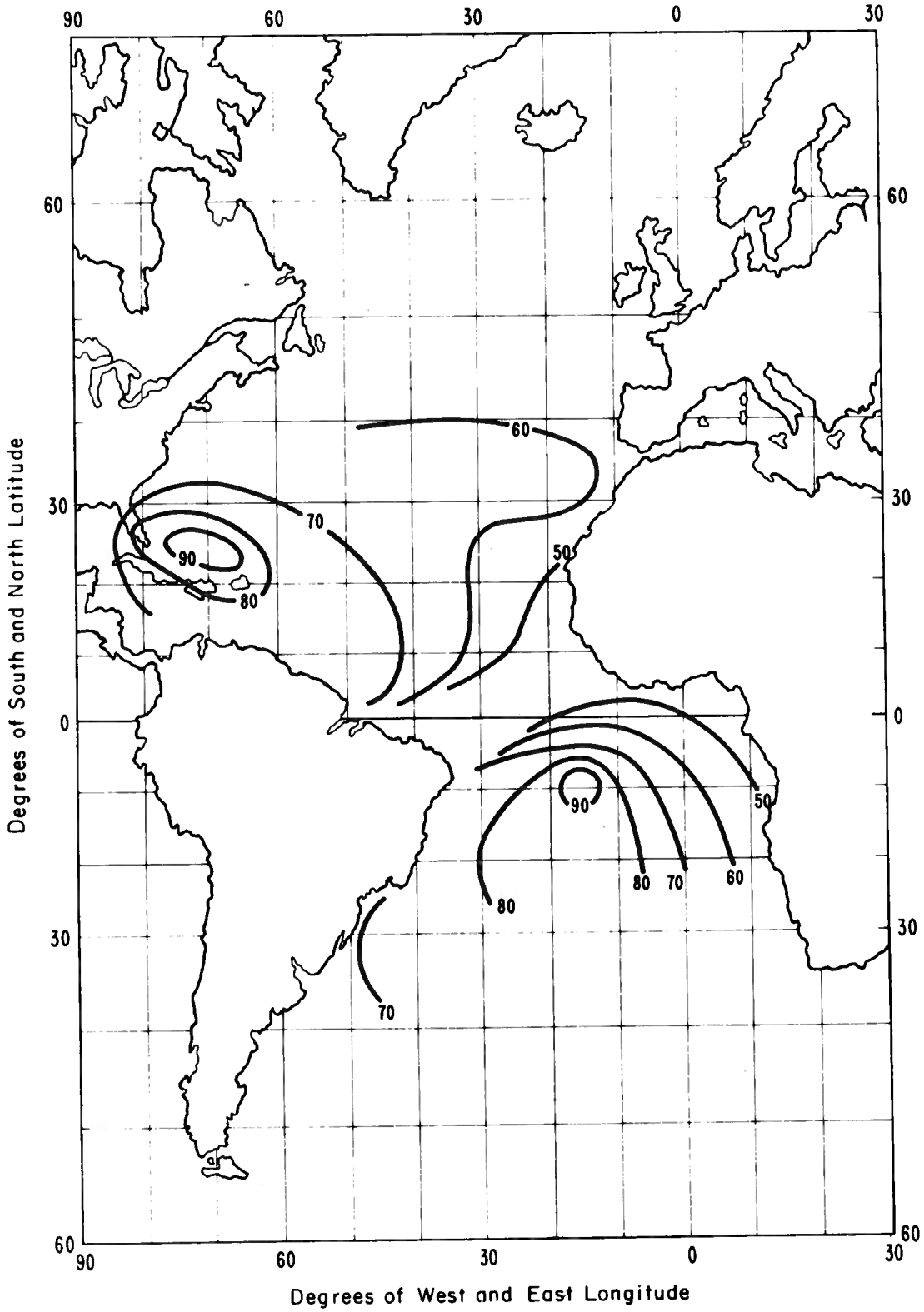

Figure 3. Percent occurrence contours for the trade wind inversion in February.

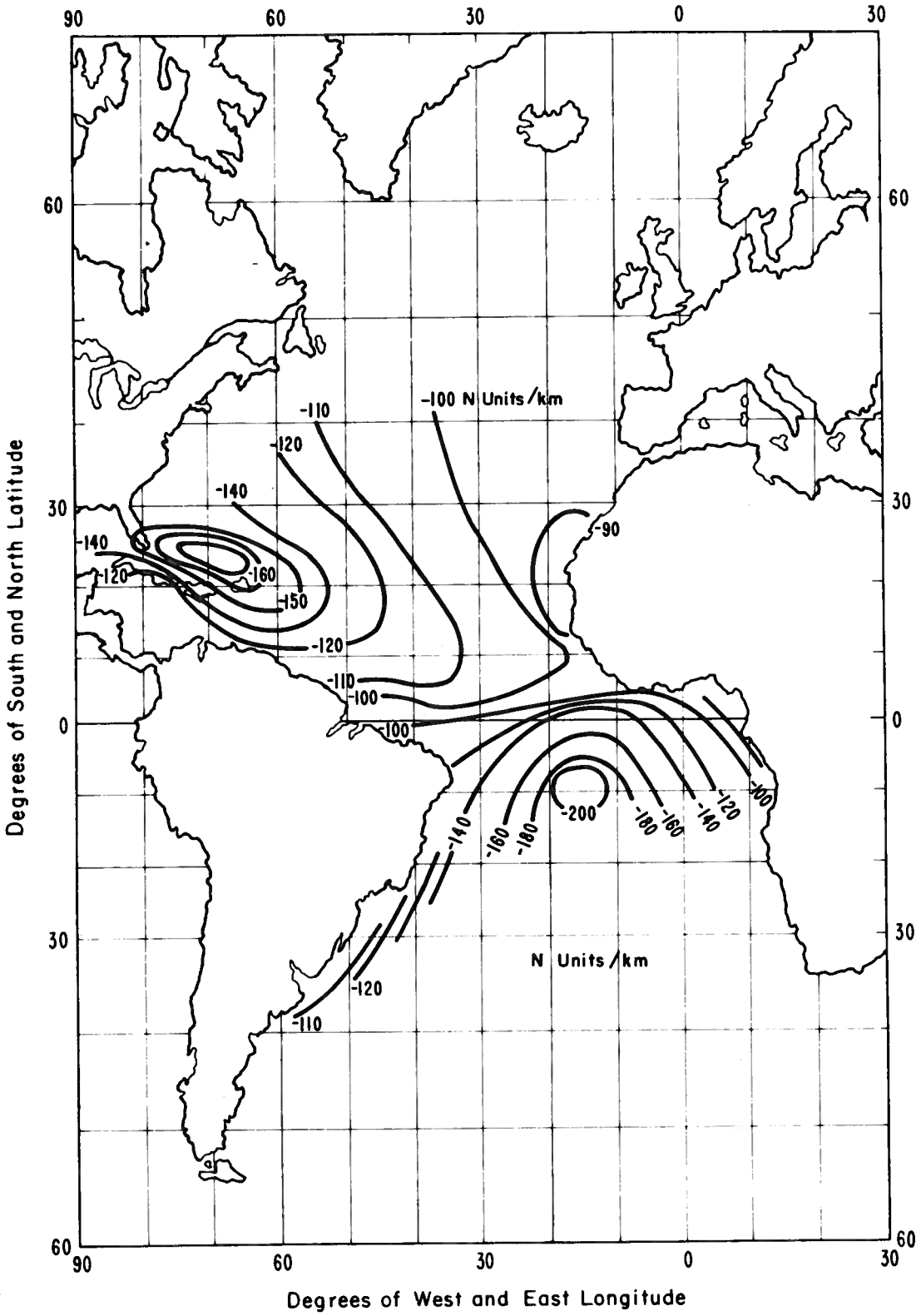

Figure 4. Contours of the mean refractivity gradient (in N units/km) for the trade wind inversion in February.

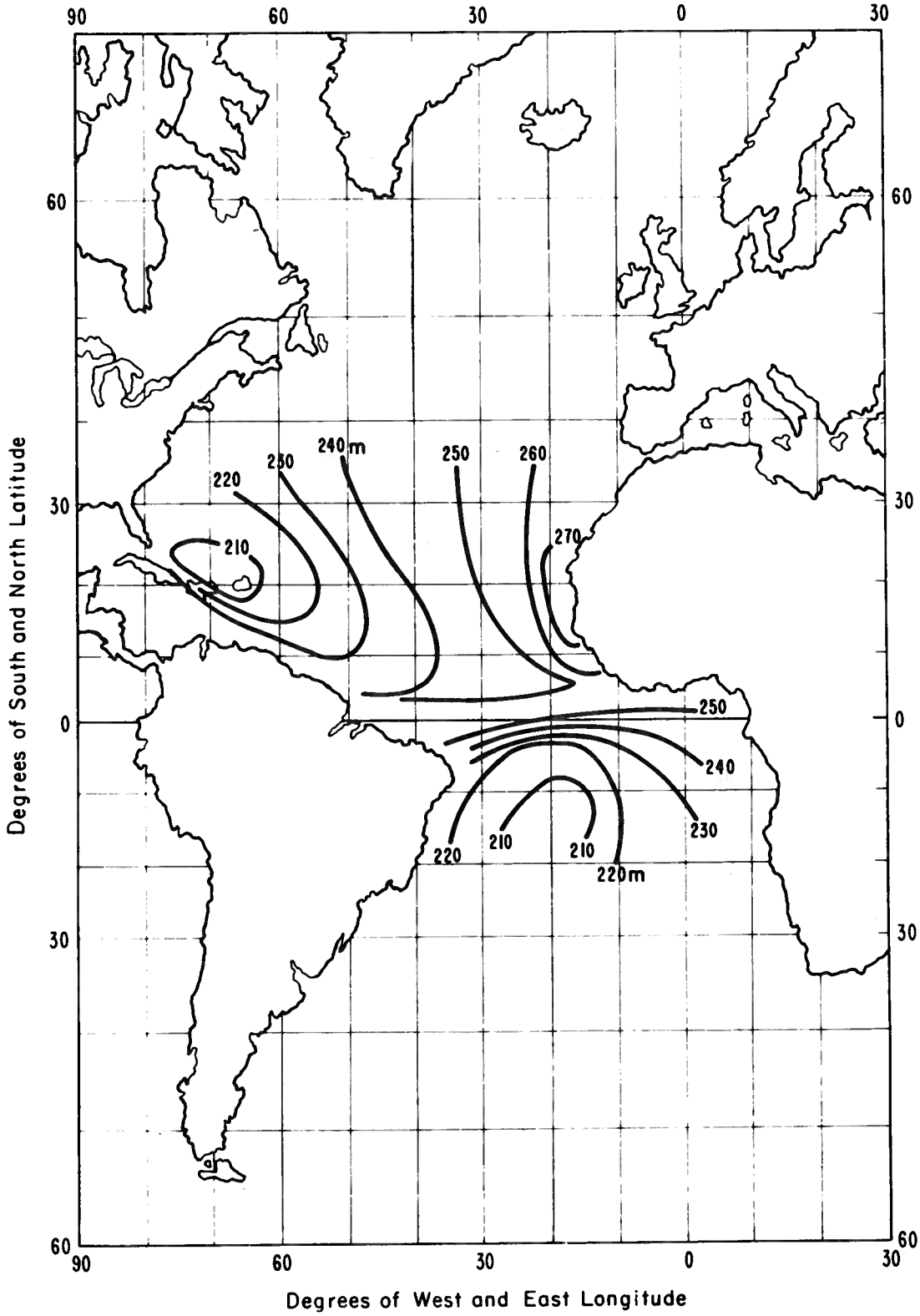

Figure 5. Contours of the mean layer thickness (in meters) for the trade wind inversion in February.

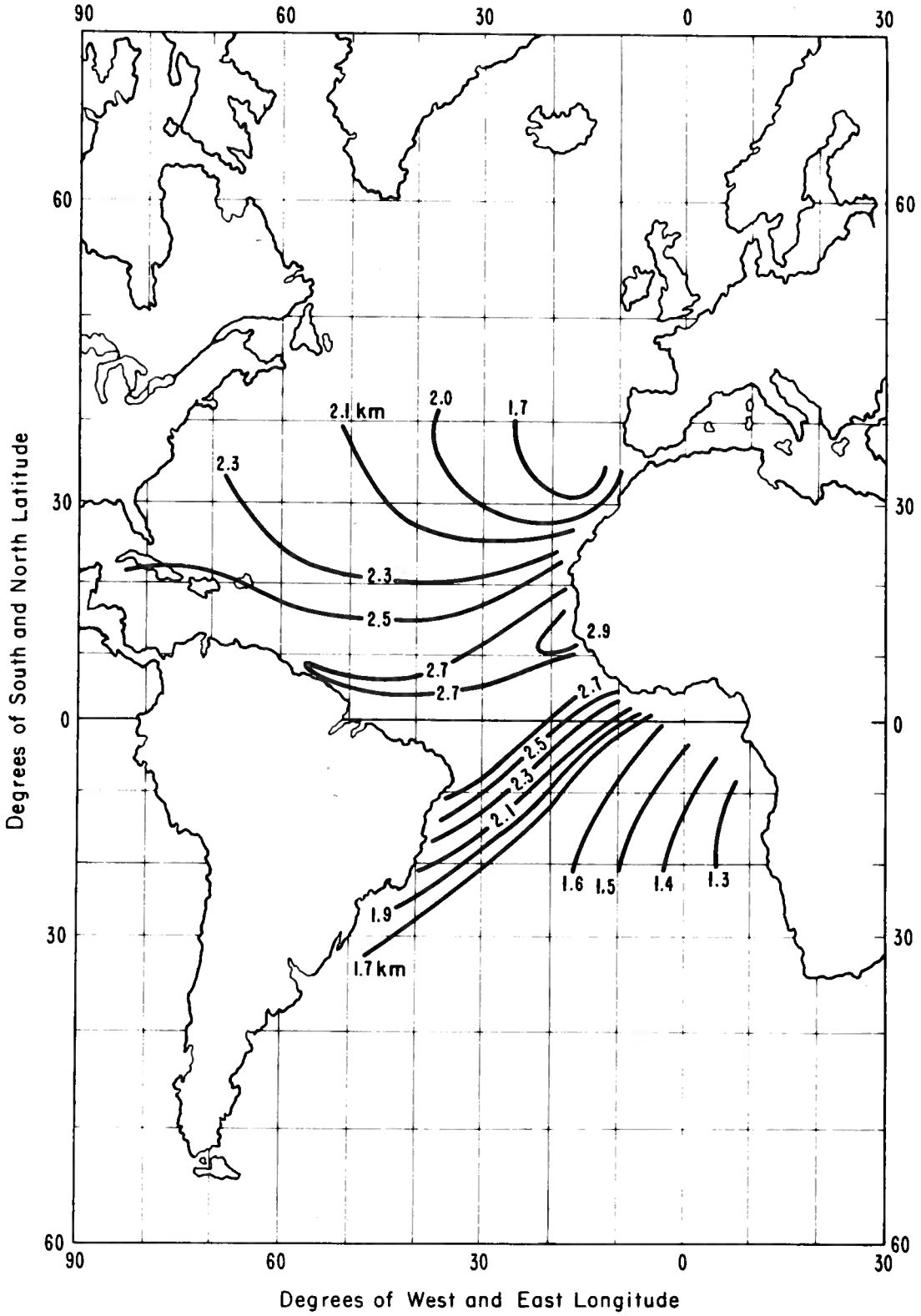

Figure 6. Contours of the mean layer base height (in kilometers) for the trade wind inversion in February.

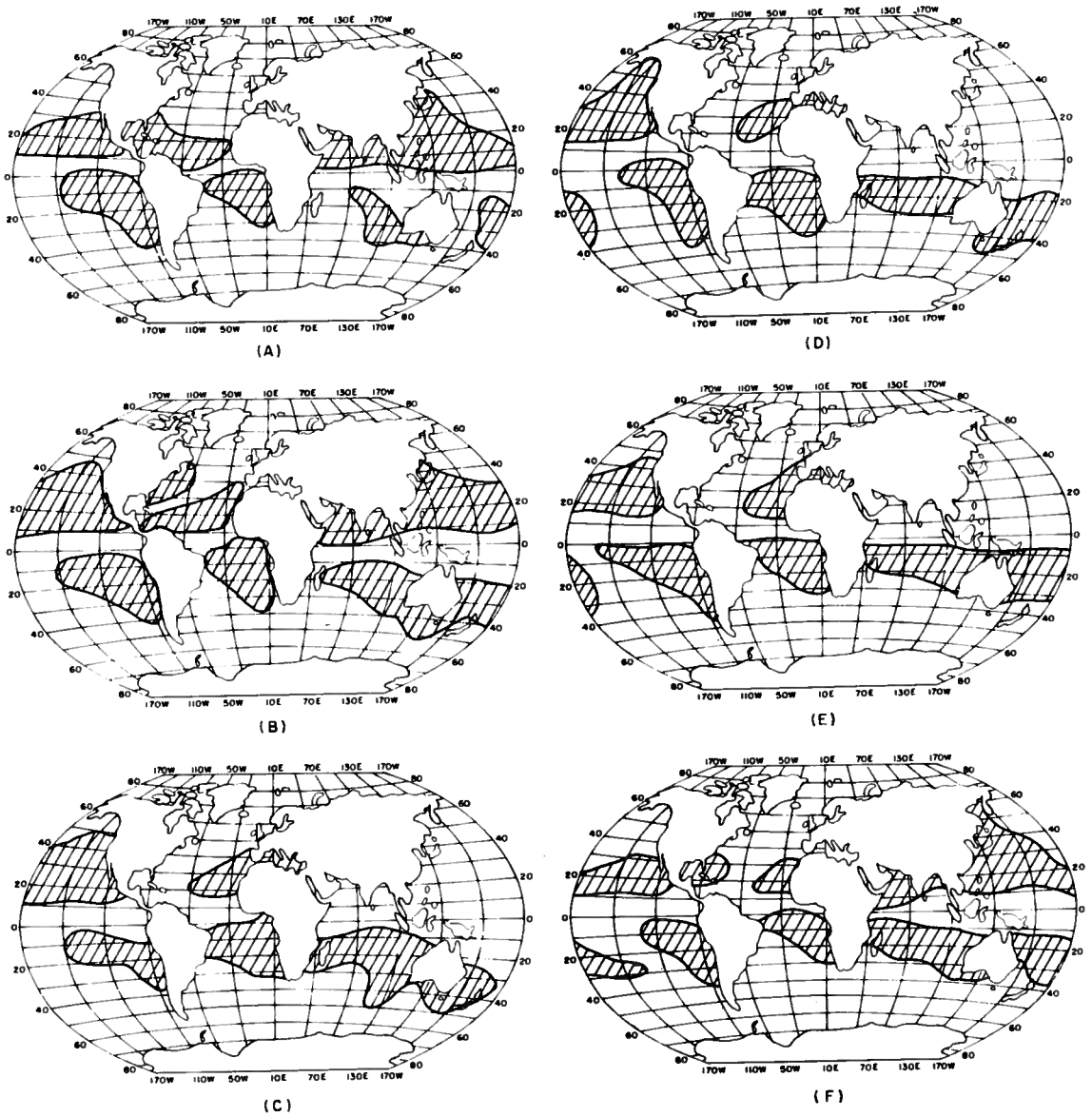

Figure 7. Areas of the world oceans where conditions are favorable for the formation of elevated layers. The charts A through F are for, respectively, January, March, May, July, September, and November (Randall, 1964).

ocean regions north of the trade wind region; see figures 7 and 8. Such layering was sufficient on one occasion to support the transmission of an excellent TV picture and sound that persisted over a 1200 mile overwater path (during broadcast hours) for more than two days.

On most overland troposcatter paths in the temperate zones, the horizontal extent of strong surface refractivity gradients is often limited by the large-scale terrain irregularities. The effect of these gradients, then, is primarily that of improving the coupling efficiency for the elevated layer mode (as indicated in figure 1 and discussed previously) rather than providing a surface ducting mode of propagation. These strong, surface, over-land gradients occur more often in the tropics than in the temperate or polar zones [Hart et al., 1971].

On the other hand, overwater troposcatter paths encounter sea-surface refractivity gradients that are more common, generally stronger, and of greater horizontal extent so that trapping can occur and be effective for greater distances. In this situation, the contribution to the coupling of an elevated-layer mode depends upon leakage from the strong surface layer. The energy that strikes the elevated layer may, therefore, be dispersed over a larger horizontal extent of the elevated layer, and in general, a less marked field enhancement can then be expected. Of course, the signal trapped by the sea-surface refractivity gradient can also contribute to the received field on transhorizon paths, but non-uniformity of the surface layer characteristics (refractivity gradient, layer thickness) can also provide a strong attenuation with distance. Marked field enhancement (via elevated layers) would therefore appear more likely in the VHF and lower SHF frequency range for the long overwater troposcatter paths.

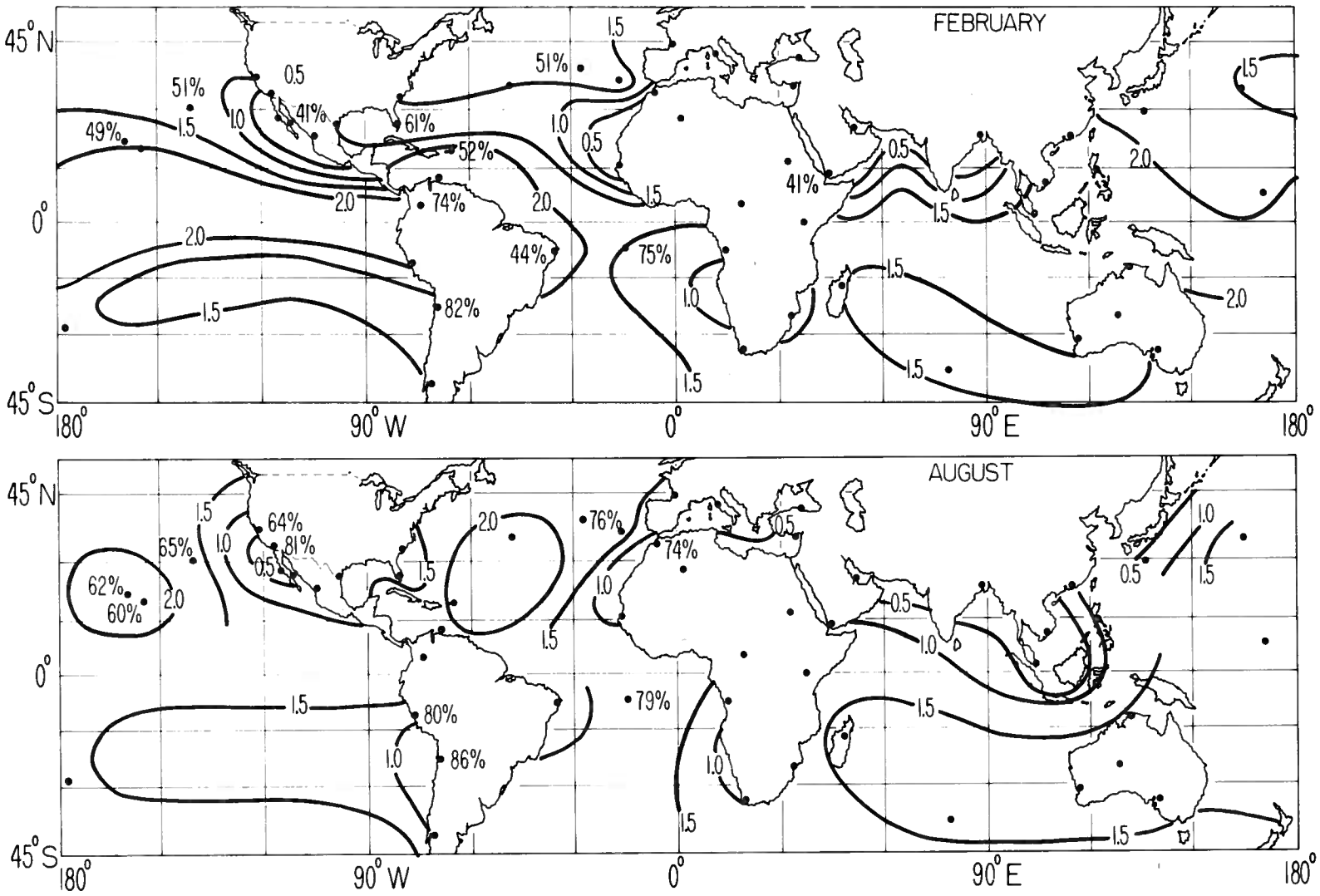

Figure 8. Mean heights (in meters) and percent occurrences (>40%) for elevated layers with gradients ≤-157.

At higher frequencies or for shorter paths, this sea-surface gradient is expected to be most effective for the enhanced fields that propagate by ducting rather than by elevated layers. This is described in Section 3.

Although the occurrence of meteorological conditions conducive to high fields (elevated layers) can be assessed for given regions of the world [Bean et al., 1966; Cahoon and Riggs, 1964; Dougherty et al., 1967; Hall 1969; Hall and Comer, 1969; Skillman, 1969], their prediction in a forecasting sense is not feasible at present.

2.3 Tropospheric Versus Sporadic-E Enhanced Fields

Many of the characteristics associated with enhanced fields via elevated atmospheric layers may be summarized as follows. The tropospheric-supported enhanced fields:

(a) have been observed for VHF, UHF, and SHF;
(b) occur for tropospheric propagation paths at distance of 150 to 700 km, and more rarely have been observed at distances in excess of 1000 km;
(c) are observed at levels which occasionally approach the free-space level;
(d) are slowly fading;
(e) are most commonly observed overwater in the tradewind regions, but are also observed overland; and
(f) are not predictable, as yet, on a day-to-day basis.

On the other hand, the ionospheric Sporadic-E layer-supported mode of enhanced fields:

(a) are observed over the HF and the VHF bands;
(b) occur for propagation paths of from 500 to 2000 km (and occasionally more) in length;

(c) are observed commonly at levels up to 10 to 20 dB below the free-space level;

(d) produce slowly fading signals;

(e) are most commonly observed in June, July, and August with a secondary, lower peak of activity in December (the enhanced fields are a daytime phenomenon in the temperate zone with a broad peak of activity centered on 1000 hours local time and frequently on a secondary evening peak around 1800 hours);

(f) are statistically predictable and exhibit a geographical pattern about the far eastern "high of activity" over Japan and the "low" over South America; and

(g) also occur, in addition to the temperate-zone mode described above, in the auroral and polar cap zones (these exhibit a temporal behavior different from the above [CCIR 1974c]).

Clearly, the occurrence of strong, slowly fading signals on very long transhorizon paths at VHF may be attributable to either atmospheric or ionospheric layering.

3. PROPAGATION VIA STRONG SURFACE DUCTS

The guiding of radio waves by the stratified atmosphere, i.e., by strong refractivity gradients at or near the earth's surface, has been long observed experimentally, and its theoretical treatment (although idealized) is advanced. These associated departures from standard propagation can be quite dramatic, particularly when associated with the refractivity structure near the sea surface. For example, marked extensions of detection range, as well as shocking reductions,

had been observed for over-water propagation dating back to World War II [Booker, 1946; Katzin et al., 1947; Unwin, 1951; Takahira and Irie, 1960; Gough, 1962; Jeske, 1964; Jeske and Brocks, 1966; Murray, 1972]. Today, there is a renewed interest in these ducted fields.

The occurrence and predictions of strong refractivity gradients has been described by Bean and his associates [Bean et al., 1966]. Although the coverage therein is nominally worldwide, it is based primarily on land stations. Their over-water summaries are based upon marine observational data from a very limited number of stations. Nevertheless, we shall concentrate on sea-surface ducts which are more prevalent and extensive than land-surface ducts.

3.1 Sea-Surface Ducting

Quantitative estimates of ducting field strengths, the radio frequencies affected, and their dependence upon antenna height are the parameters whose prediction is of interest. These are, of course, all functions of the sea-surface refractivity gradient (its strength, vertical extent, and horizontal continuity), which can vary with time of day and year or the distribution of weather elements. In general, the superrefractive sea-surface layers ($\Delta N/\Delta h \leq -157$ N units/km) are of interest since they are normally favorable to radio wave propagation. This assumes the radio path terminals are both well immersed in the superrefractive layer; otherwise, the duct efficiency is reduced. The effect of the layer can even be detremental to radio wave propagation. See figure 9; the position of the propagation path terminals relative to the duct boundary is critical [Bean and Dutton, 1968; Dougherty, 1968]. That is, the operable mode of propagation between two telecommunication terminals in the presence of a surface layer may be effectively that of line-of-sight, beyond the horizon,

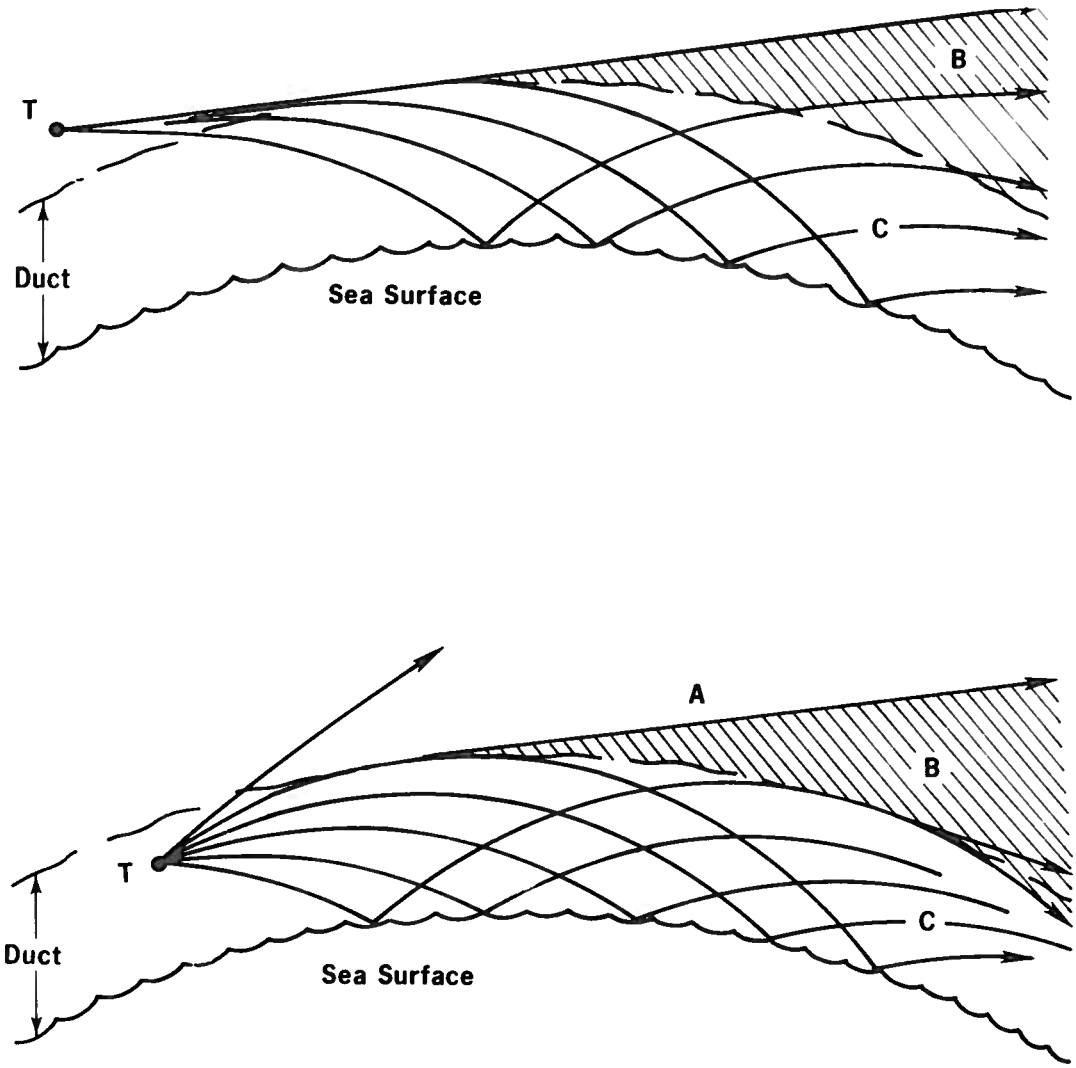

Figure 9. Identification of the propagation mode for locations of a transmitter above the duct (top drawing) and within the duct (bottom drawing). Reception in regions A, B, and C is via, respectively, the line-of-sight, beyond-the-horizon (diffraction or leakage), and ducted modes of propagation.

or ducted propagation, depending upon the location of the terminals relative to the vertical extent of the layer.

Therefore, one useful categorization of superrefractive layers would be in terms of their vertical extent. Deep layers (extending to 25 m or more above the surface) would be relevant to ocean vessel communication; communication antennas have been at about 24 m above the sea on most naval vessels, and search radars on capital ships have been at about 30 m above the sea. On the other hand, shallow layers (extending up to 15 m or less) would have significance for propagation between terminals (communication terminals or low-sited radars) on smaller craft. For the prediction of sea-surface layers, a preferable classification may be that of the meteorologists who categorize atmospheric layers in terms of their dominant causative mechanism. Fortunately, this latter classification approximates the former; advection-type layers tend to be deep, and evaporation-type layers tend to be shallow.

3.2 Superrefractive Advection Layers

The deep, superrefractive ($\Delta N/\Delta h < -157$ N units/km) advection layers result from the movement of warm dry air over the sea [Bean et al., 1966]. For example, during the late summer and early fall, the prevailing winds move continentally modified (warm dry) air masses offshore over cooler maritime air. As a result, favorable locations for the occurrence of these advection layers border the coasts of continents or large islands. Some such locations are:

- the coastal waters of the Gulf of Mexico and the Baltic Sea;
- the coastal waters near the North Atlantic States, Newfoundland, and Great Britain (especially in the North Sea);

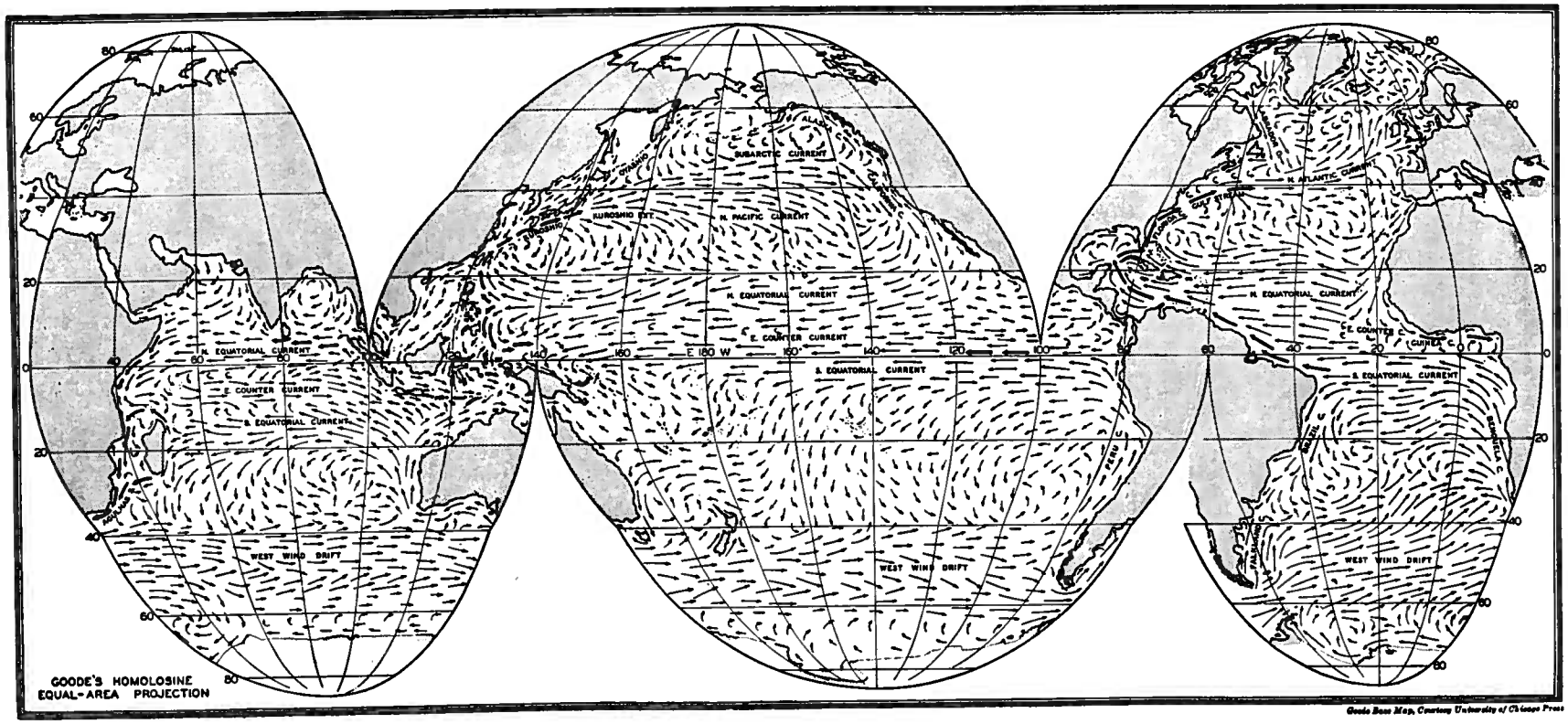

Figure 10. Surface currents of the oceans in February-March [Sverdrup, 1943].

- leeward of the islands of Japan, islands in the Caribbean Sea, and islands in Indonesia; and
- the waters of the Red Sea, the Gulf of Aden, the Persian Gulf, and the Arabian Sea (in the months immediately preceding and following the monsoon season).

Similarly, the circulation patterns of air and ocean combine to produce advection layers near the sea surface. For example, large oceanic semi-permanent highs are characterized at lower elevations by a large mass of air which has warmed and dried adiabatically during its descent. Therefore, superrefractive advection layers also occur near the west edge of continents, at latitudes of approximately 15° to 35° N or S, where the eastern section of a semi-permanent high tilts down toward the sea surface in the vicinity of a cold ocean current (in figure 10, the cold ocean currents are those between 40°N and S and moving toward the equator). Favorable locations for these advection layers are, therefore, the coastal waters:

- near Southern California and the Baja Peninsula, (mostly in winter),
- near Peru and Chile,
- near west Africa (15° to 22° N or S in winter),
- near west Australia in summer, and
- in the eastern Mediterranean Sea (in summer).

3.3 Evaporation Layers

Shallow superrefractive evaporation layers are found over extensive areas of the ocean, whenever conditions are conducive to rapid evaporation rates. These layers result primarily from the humidity-temperature contrasts between air and sea in a shallow transition layer adjacent to the surface. In addition, the evaporation rate per unit area and, consequently, the

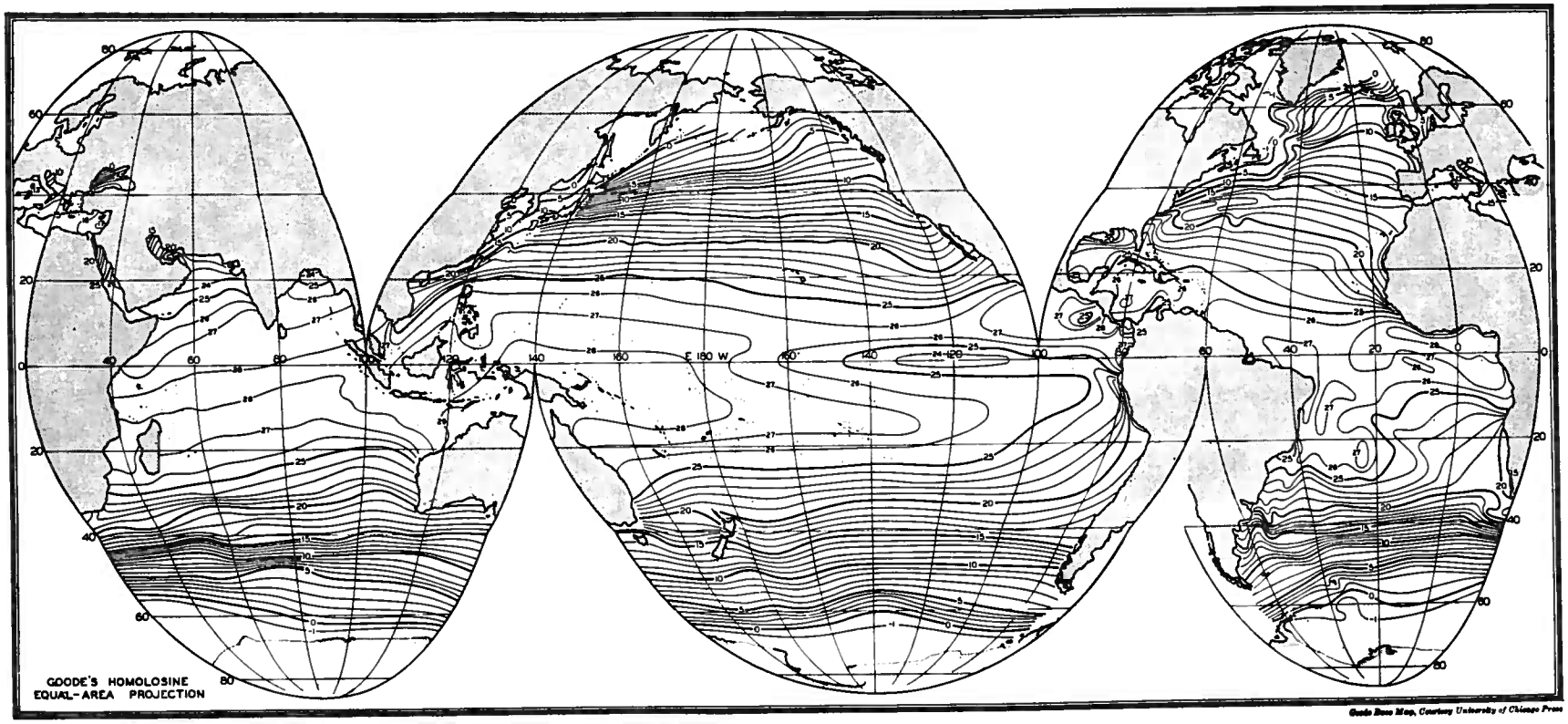

Figure 11. Surface temperatures of the oceans in February [Sverdrup, 1943].

occurrence and strength of these layers is strongly influenced by the speed and steadiness of the local wind.

The strongest evaporation rates are found north of 35°N (or south of 35°S) in winter over warm ocean currents such as the Kuroshio (Japan), the North Atlantic Drift, the Alaskan Current and the East Australian Current; see figure 10. In middle latitudes the amount of evaporation per unit area varies with the seasons, reaching a minimum in summer (June and July in the Northern Hemisphere) and a maximum in the fall and early winter (September, October, and November in the Northern Hemisphere) when, although the air is cold, the water is still relatively warm; see figures 11 and 12 [Sverdrup, 1943].

In the tropics, evaporation takes place all of the time, since the sea-surface temperature is normally higher than that of the air above it. However, because this difference in temperature (and in the corresponding absolute humidity) is small, the actual rate of evaporation per unit area is not as great as in the middle latitudes, but the resulting shallow superrefractive layer can be very intense. These strong evaporation layers are reported as a semi-permanent feature in the Caribbean, disrupted by, and reforming immediately after, the passage of squall lines [Katzin et al., 1947]. Other tradewind areas, where evaporation exceeds precipitation (see figure 13), are also likely regions for strong evaporation layers [Gentilli, 1958].

All oceans experience fluctuations in the evaporation at certain periods and in certain regions; these appear to be related to the persistence of anomalies in the monthly and yearly sea-surface temperatures. Anomalies also occur in the humidity or water vapor structure, but conclusive determination of humidity fluxes over the sea is still lacking (Fleagle, 1970; Miyake and Donelan, 1970). Superrefractive layers are sometimes associated with steam fog or "Arctic smoke," although this is usually an indication of the onset of the layer's disintegration.

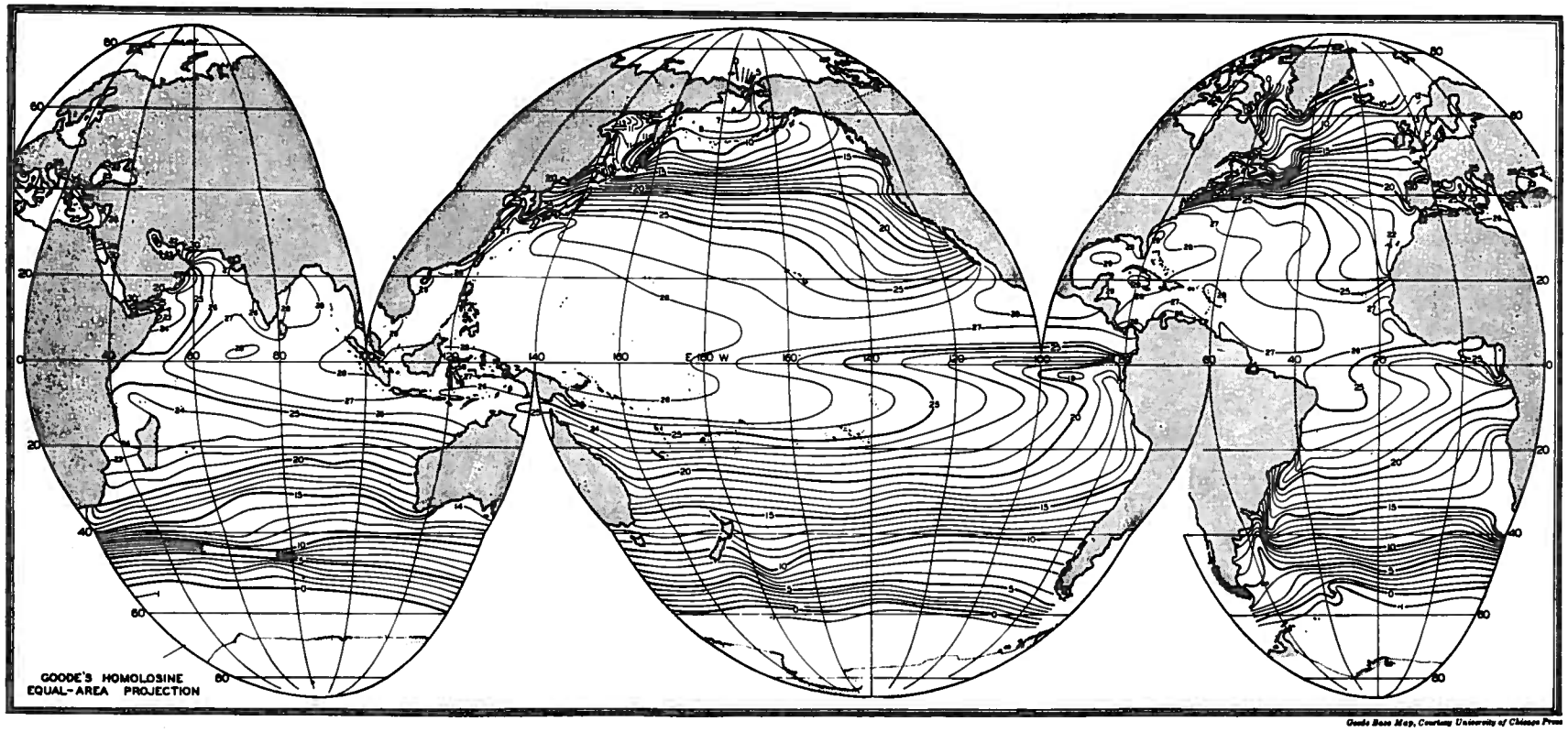

Figure 12. Surface temperatures of the oceans in August [Sverdrup, 1943].

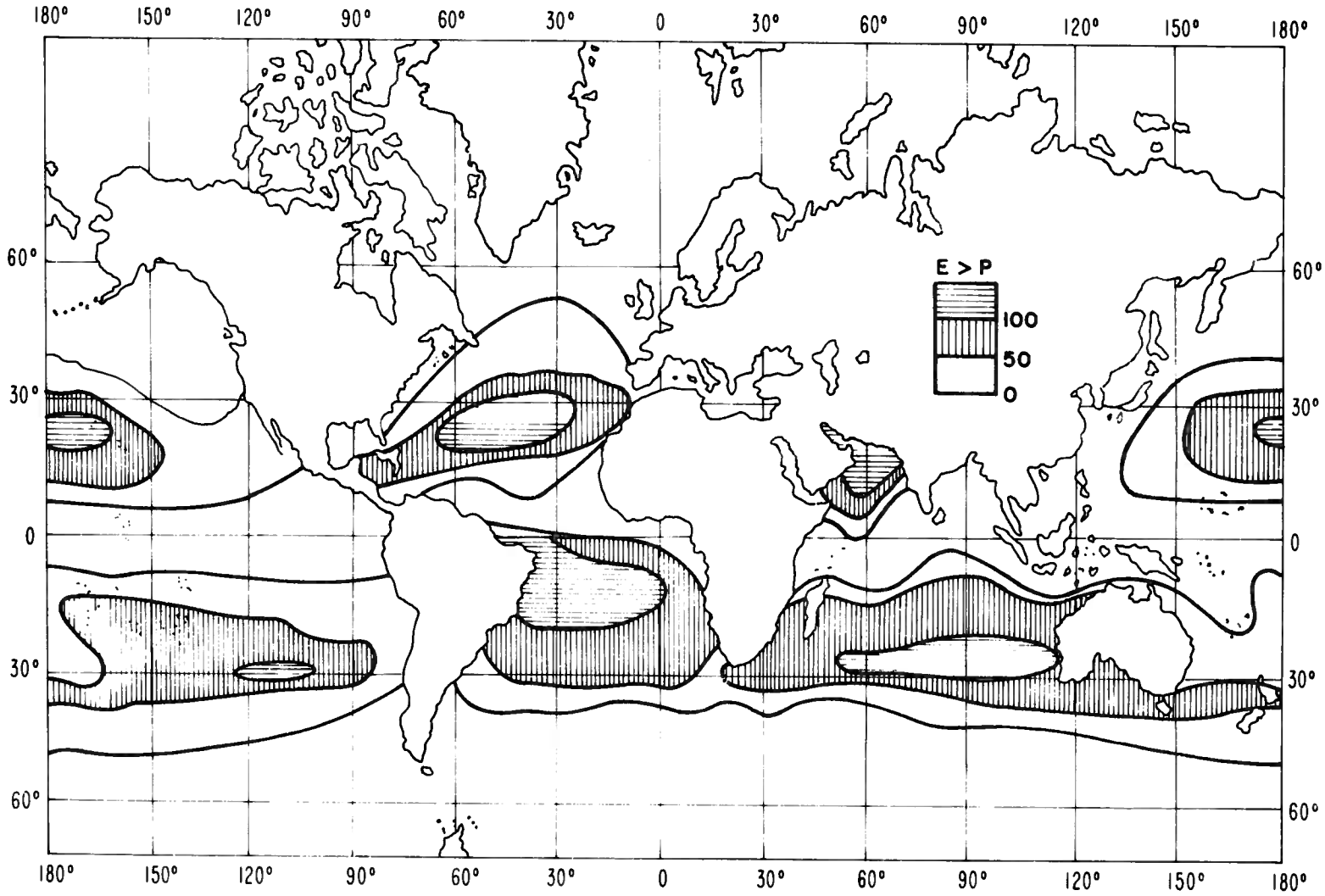

Figure 13. Areas of the world where evaporation exceeds precipitation. The estimated difference is given in centimeters per year [Gentilli, 1958].

3.4 Subrefractive Advection Layers

Superrefractive layers provide a curvature to the radio wave path in the same sense as that of the earth, so that the distance to the radio horizon over the sea normally exceeds that to the geometric horizon. For subrefractive layers, however, the curvature of the radio path is in the opposite sense; the distance to the radio horizon over the sea would then be less than that to the geometric horizon. Subrefractive layers are, therefore, generally detrimental to radio wave propagation. They also provide an internal reflection of radio waves [Wait, 1969].

These subrefractive layers have not been studied in great detail but could occur wherever warm moist air overlies a cooler sea surface (with both air and sea surface temperatures greater than 10°C). If a local water-vapor inversion (an increase of water vapor with height) results, fog, subrefraction, or both can be produced. This advection fog results when the lowest layers of the atmosphere are cooled to the saturation point by the cooler ocean waters, but fog and subrefraction seldom occur together for prolonged periods because, as the fog intensifies, the condensation process weakens the subrefractive gradient.

The ocean areas particularly susceptible to this subrefractive and/or fog formation would lie between 45°N and 40°S where prevailing winds transport nearly-saturated air from the vicinity of a warm ocean current to the vicinity of a cold ocean current. These would be areas where warm and cold currents adjoin or even converge (see figure 10). In August or September, areas favorable for these subrefractive layers in the Northern Hemisphere would be the Gulf of Guinea in Africa and the coastal waters:

north and south of Great Britain,
west of Nova Scotia and Newfoundland,
north of Hawaii,
east of China and Indochina,

near Arabia, and
west of Central America.

In February or March, favorable locations in the Southern Hemisphere would be the coastal waters:

near the larger Indonesian Islands,
north of New Zealand,
between Madagascar and Africa,
southeast of South America, and
east of Australia.

Observations of sea-surface subrefractive gradients determined from ship-bridge heights may actually be a measure of slightly elevated subrefractive layers, beginning a few meters above the surface and extending vertically 50 m or more. Coastal stations along shallow waters warmed to about 30°C (e.g. at Tampa, Florida) may show surface subrefractive layers; however, this surface subrefraction would be found only on the coast; a corresponding layer over the water may overlie a superrefraction sea-surface evaporation layer.

3.5 Overwater Prediction Charts

The foregoing demonstrates how an understanding of the causative physical processes permits an identification of the ocean areas favorable for the occurrence of superrefractive or subrefractive layers. This is essential if the meteorological data obtained from the very limited number of marine observational stations are to be extrapolated over the oceans of the world. In addition, quantitative estimates of certain layer characteristics are necessary, for radio propagation prediction purposes. Although these characteristics of interest (the strength of the gradient, its vertical and horizontal extents, and its occurrence) are not adequately measured at present, some estimates are available.

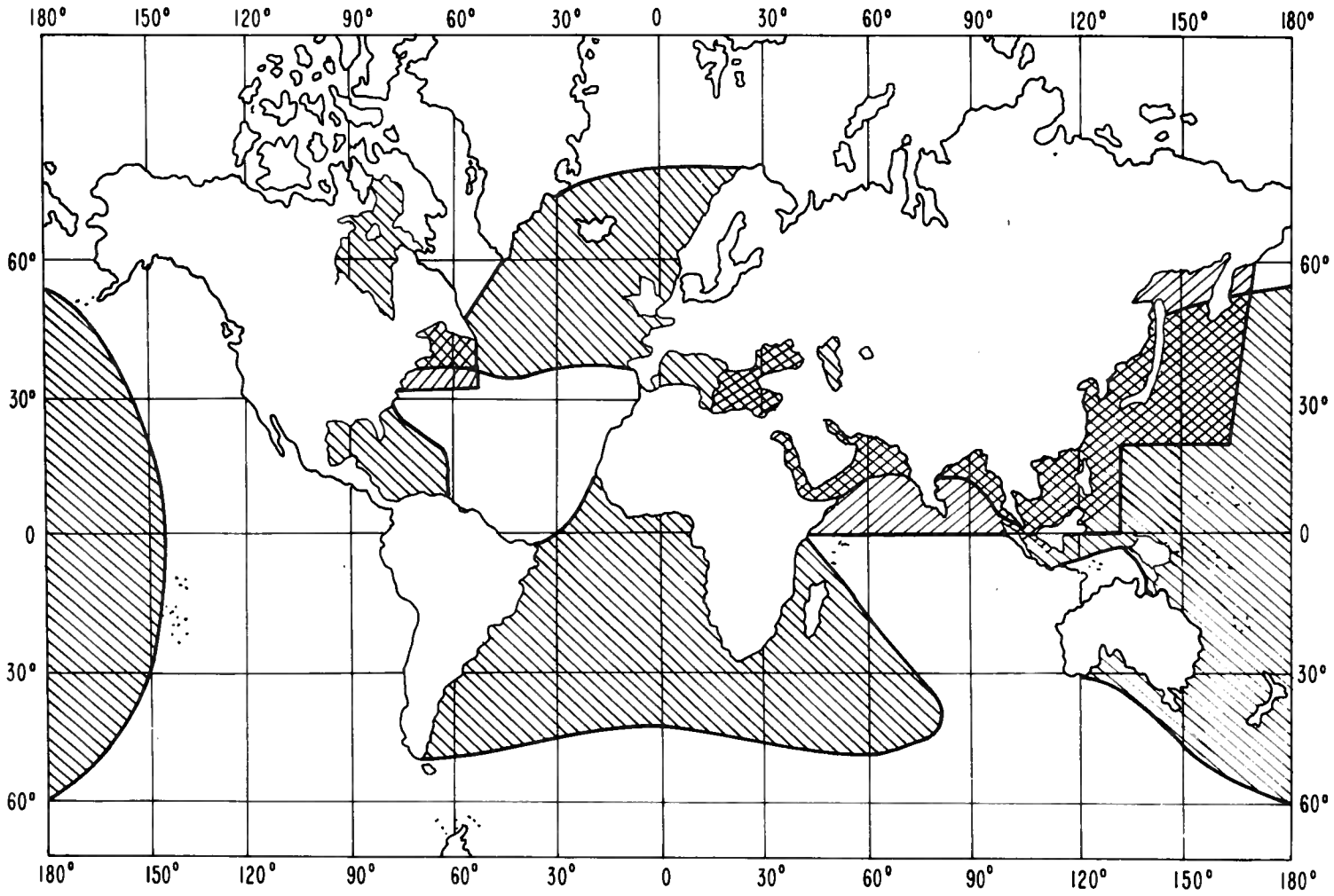

Figure 14. Regions for which charts are available primarily of advective layers ▨ and primarily of evaporative layers ▧ .

Figure 14 indicates those world oceanic areas for which estimates are available of the characteristics of subrefractive and superrefractive layers. These represent a substantial beginning but further estimates are necessary; estimates of the diurnal variation of the layer characteristics are particularly limited. The ocean areas of figure 14 with the diagonal shading //// are those for which charts, primarily of advection layers, are available. The ocean areas with the reverse diagonal shading are those for which charts, primarily of evaporation layers, are available.

A particularly useful type of prediction chart, illustrated in figure 15, gives the percent expectancy of extended ranges (50% or greater increase in range) for L, S, and X-Band Radar for superrefractive ($\Delta N/\Delta h < -157$ N units/km) layers. Similar charts appear in Crozier, et al. [1952], USNEL [1952], Cowan [1953], Gossard and Anderson [1956a, 1956b], Gossard [1957 and 1964], Holden et al. [1960], Ikegami [1964] and Nookester and Hitney [1974]. These are actually charts determined from the potential refractive index observed at ship-bridge heights and under various wind conditions. For an assumed height distribution of refractive index, these variables permit an estimate of the sea-surface-layer refractivity gradient and its vertical extent. Those variables associated with super-critical gradients are then combined into one convenient parameter, the "maximum-trapped-wavelength", that results from Schelkunoff's solution [1944] of the simplest guided-wave propagation problem. Although this maximum trapped wavelength is only an approximation, it does serve as a convenient parameter for charting the multiplicity of surface-layer characteristics pertinent to propagation via the sea-surface (super-critical) duct.

Similar seasonal charts, illustrated in figure 16, are available for advection layers and for frequencies less than 300, 1000, and 3000 MHz [Bean et al., 1966]. Also available

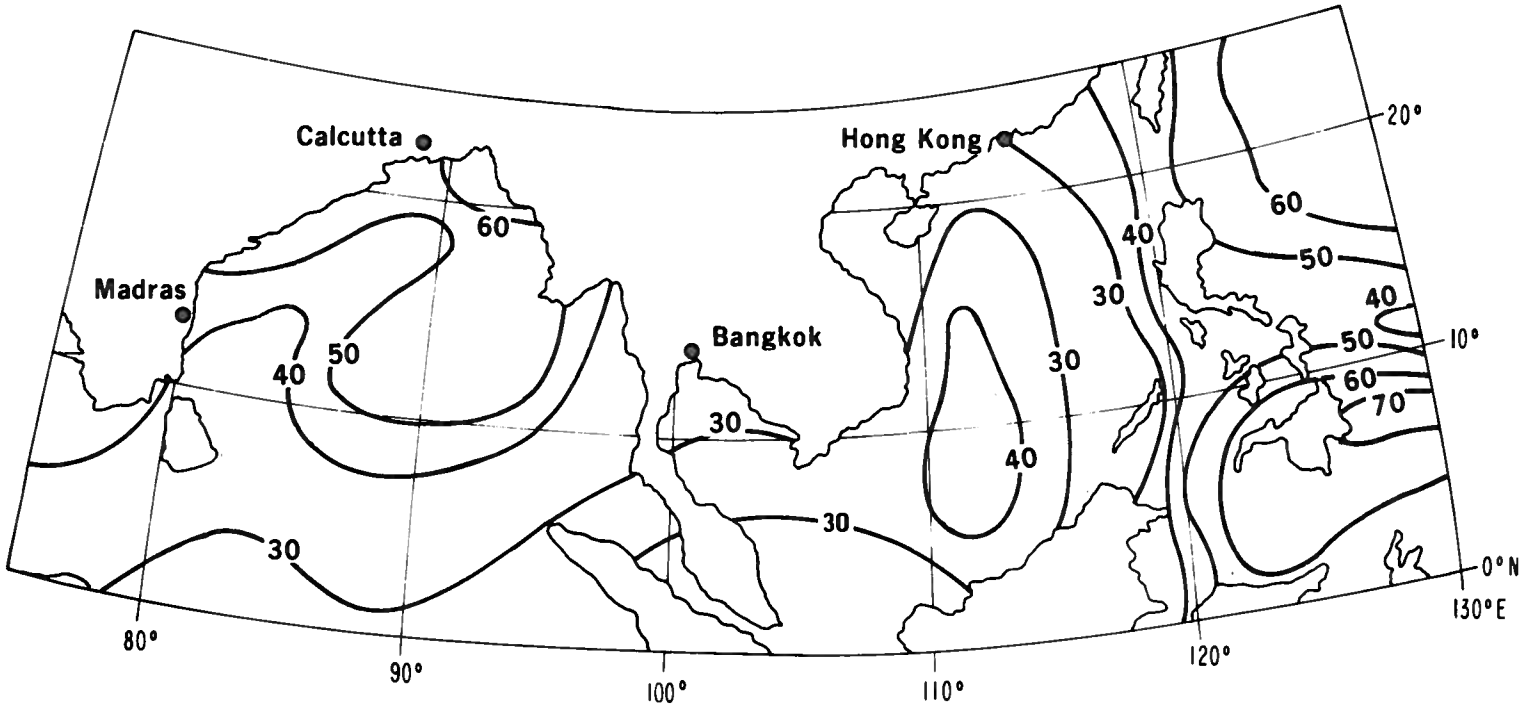

Figure 15. Percent expectancy of extended coverage, S-band radar, Southeast Asia, January [Gossard and Anderson, 1956a].

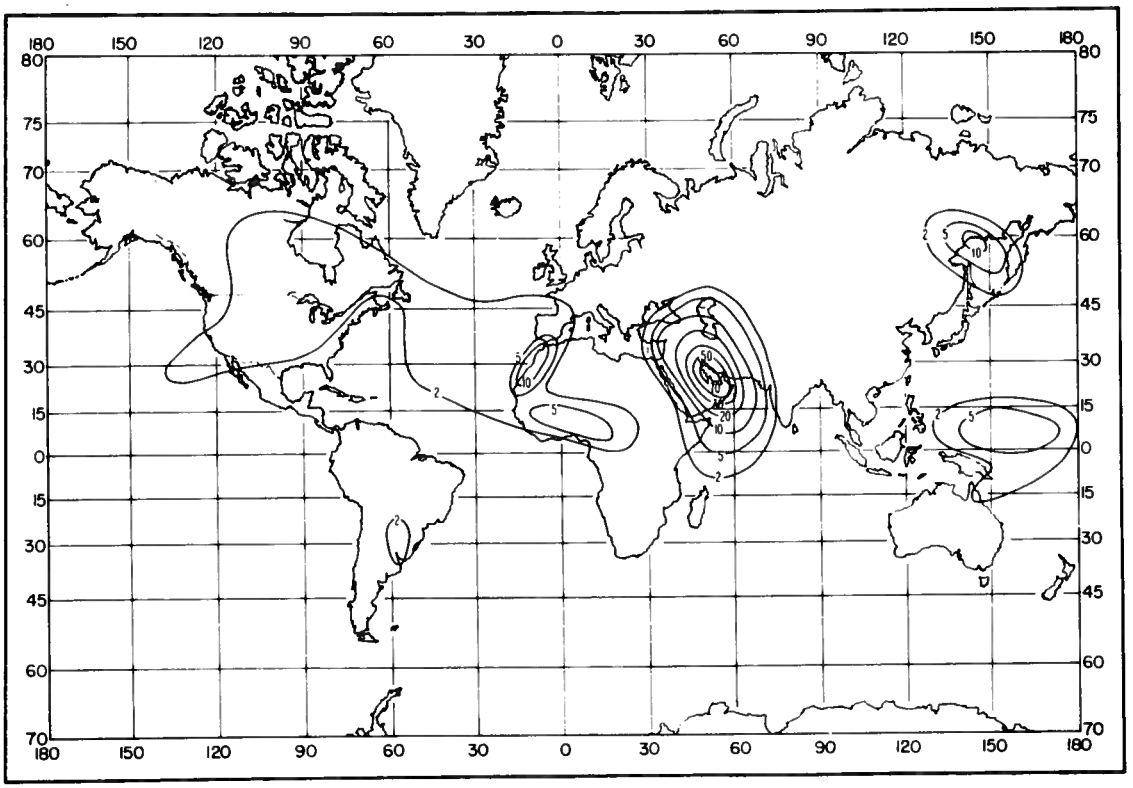

Figure 16a. Percent of time trapping frequency <300 MHz, August.

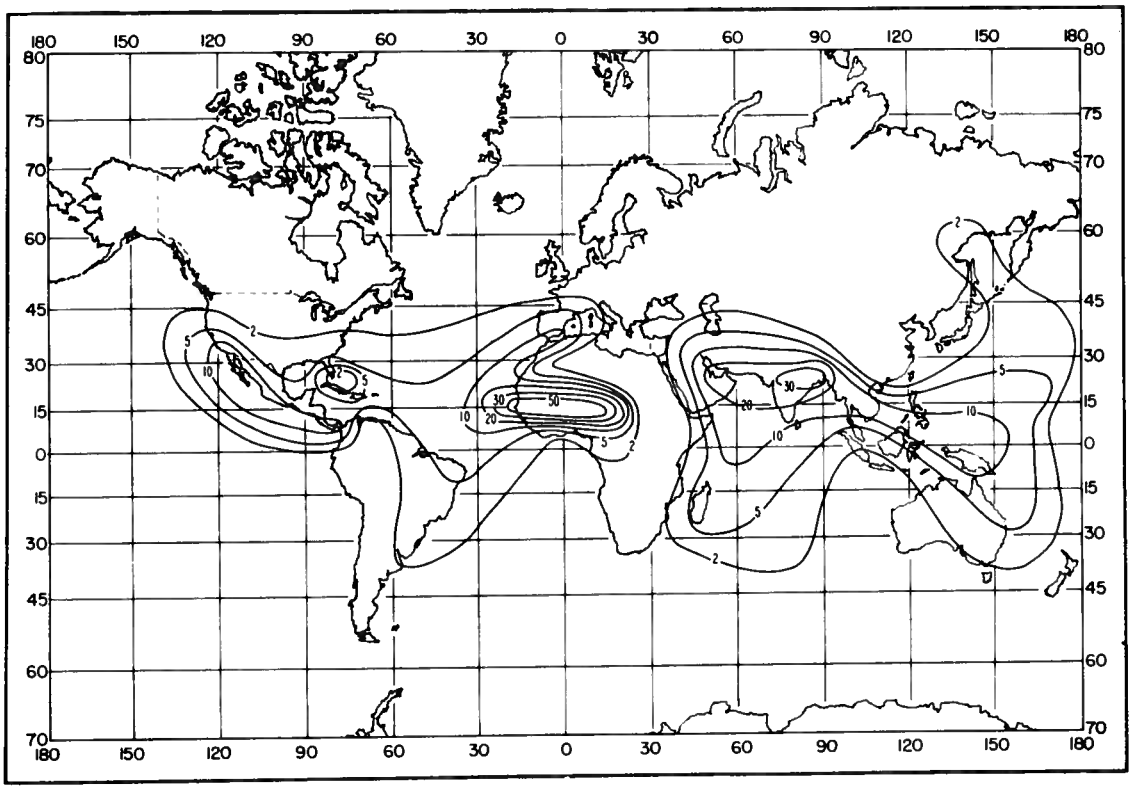

Figure 16b. Percent of time trapping frequency <3000 MHz, November.

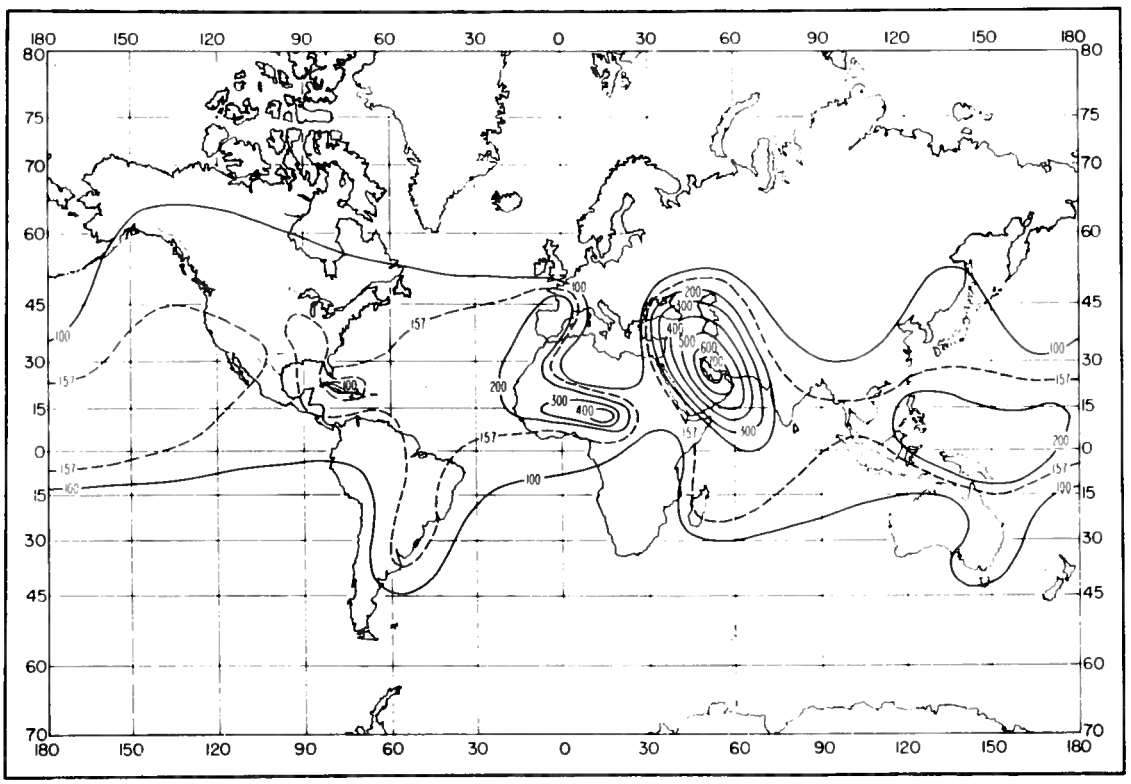

Figure 17a. Refractivity lapse rates (N/km) not exceeded 5 percent of time for 100 m layers, August.

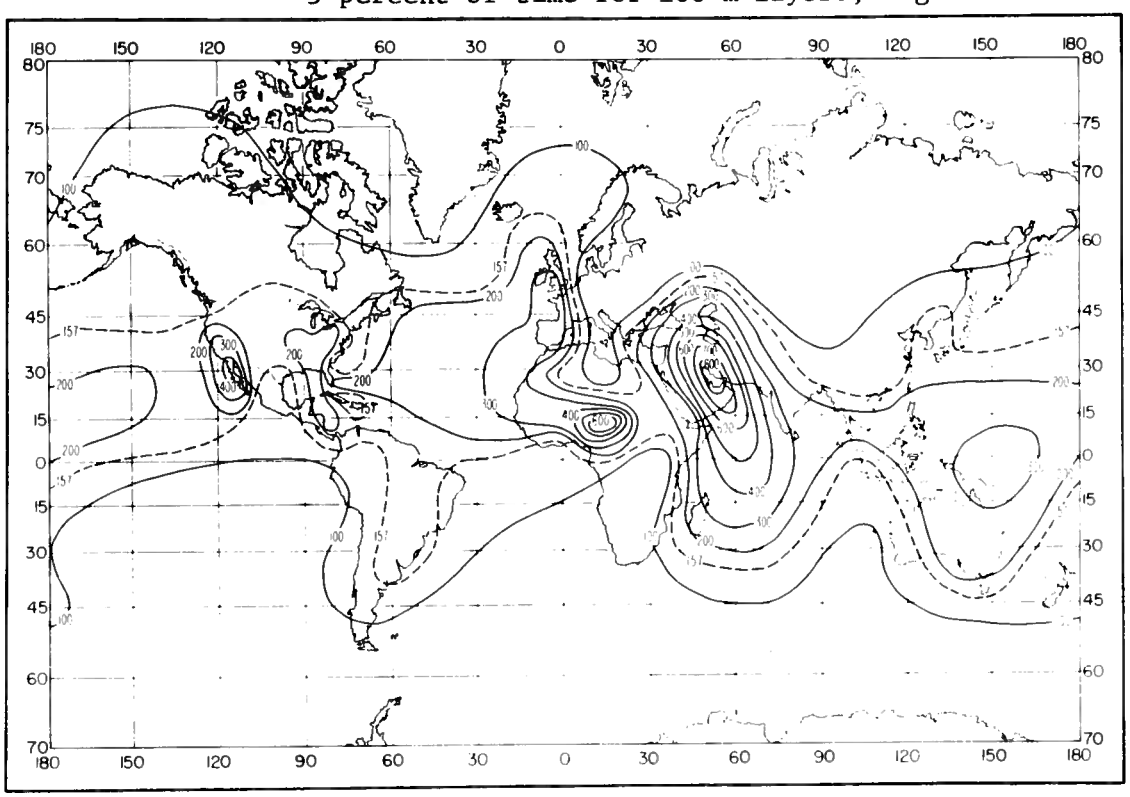

Figure 17b. Refractivity lapse rates (N/km) not exceeded 2 percent of time for 100 m layer, August.

are various graphical techniques for estimating duct intensities and the possibility of extended coverage for specific locations from on-site observations (Anderson and Gossard, 1952, 1955; USNWSC, 1967; Wickerts, 1970).

Additional charts are available for the characteristics of advection-type layers during the seasons typified by the months of February, May, August, and November and over most of the world's oceans [Bean et al., 1966]. These world charts include:

- the percent of observations for which the surface gradients are subrefractive, superrefractive, or supercritical;
- those gradients (averaged for 100 m above the surface) exceeded for 2 and 10 percent of the observations;
- those (100 m) gradients not exceeded for 2, 5, 10, and 25 percent of the observations; and
- the percent of superrefractive and supercritical gradients that extend more than 100 m above the surface.

Figures 17 and 18 illustrate some of the above charts; the lapse rate is the negative of the gradient. Seasonal distributions are also available for selected North Temperate Zone locations, as illustrated by figures 19 and 20 [Samson, 1975]. For tropical locations, the seasonal means are less informative, since there tends to be wide diurnal variations in the surface gradients. This is illustrated by figure 21 [Hart et al., 1971]. The arrows at the base of the charts in figure 21, indicate gradients more negative than -1000 N units/km.

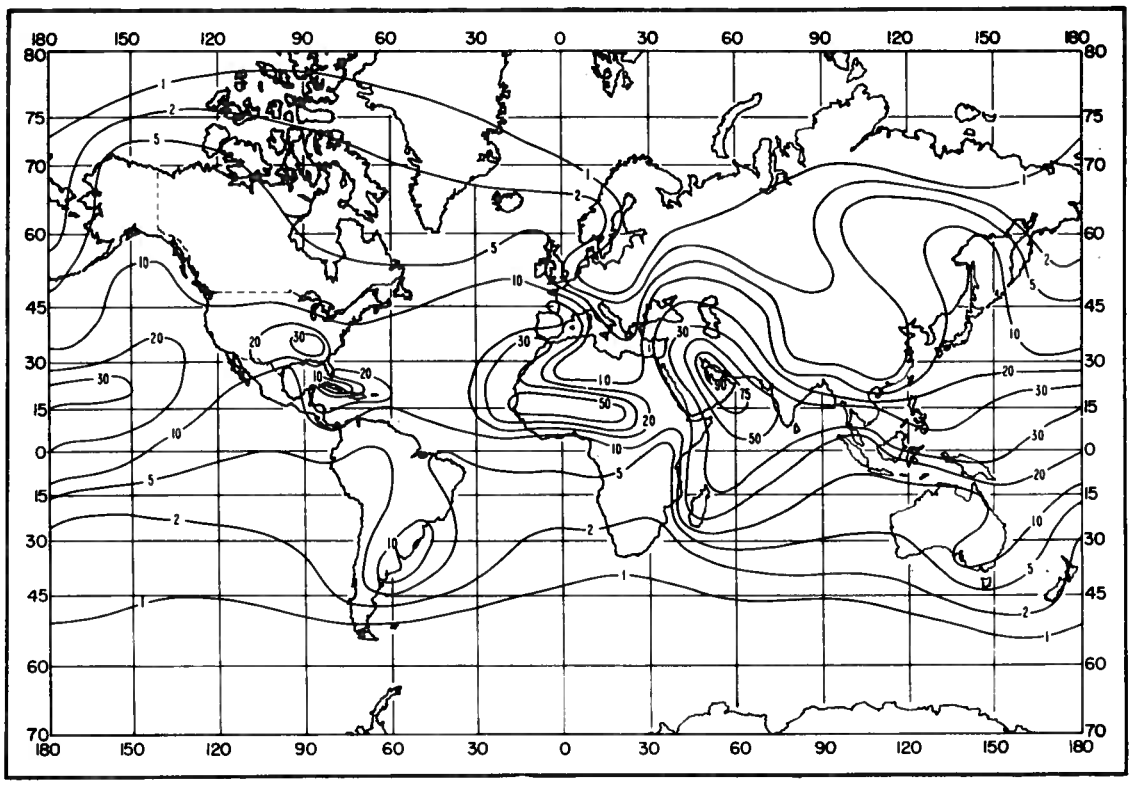

Figure 18a. Percent of time gradient ≤-100 (N/km), August.

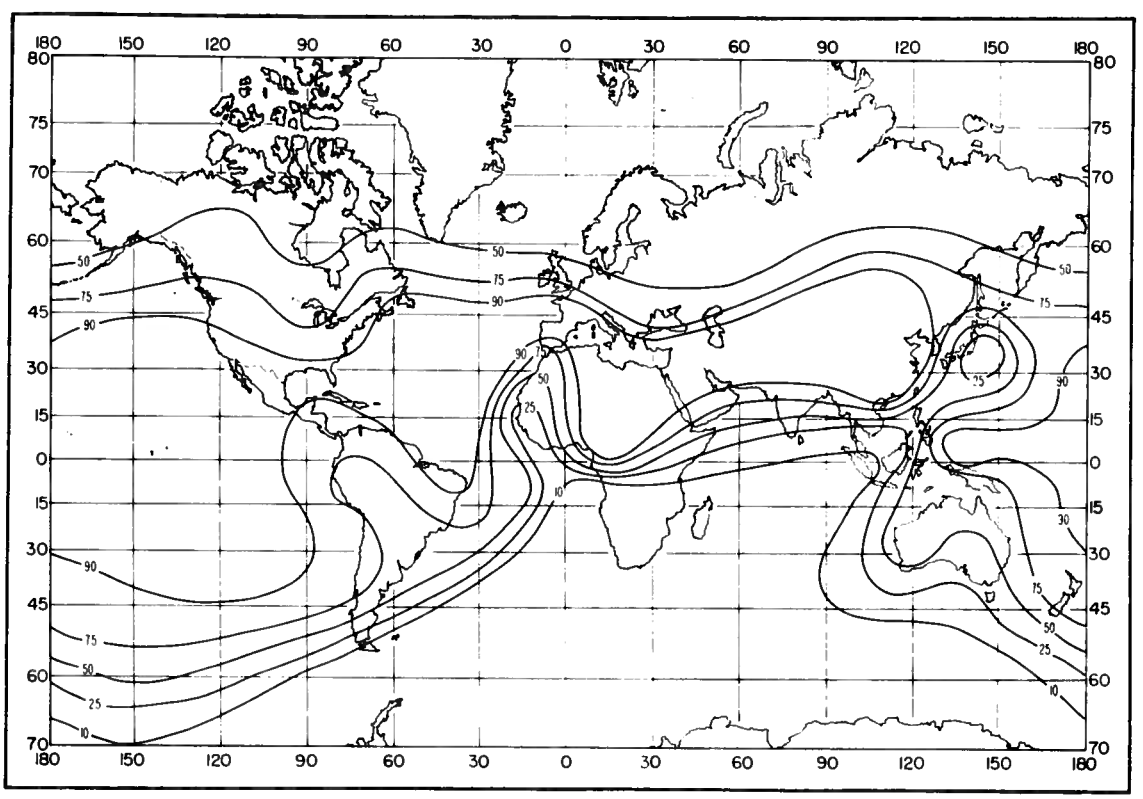

Figure 18b. Percent of superrefractive layers thicker than 100 m, August.

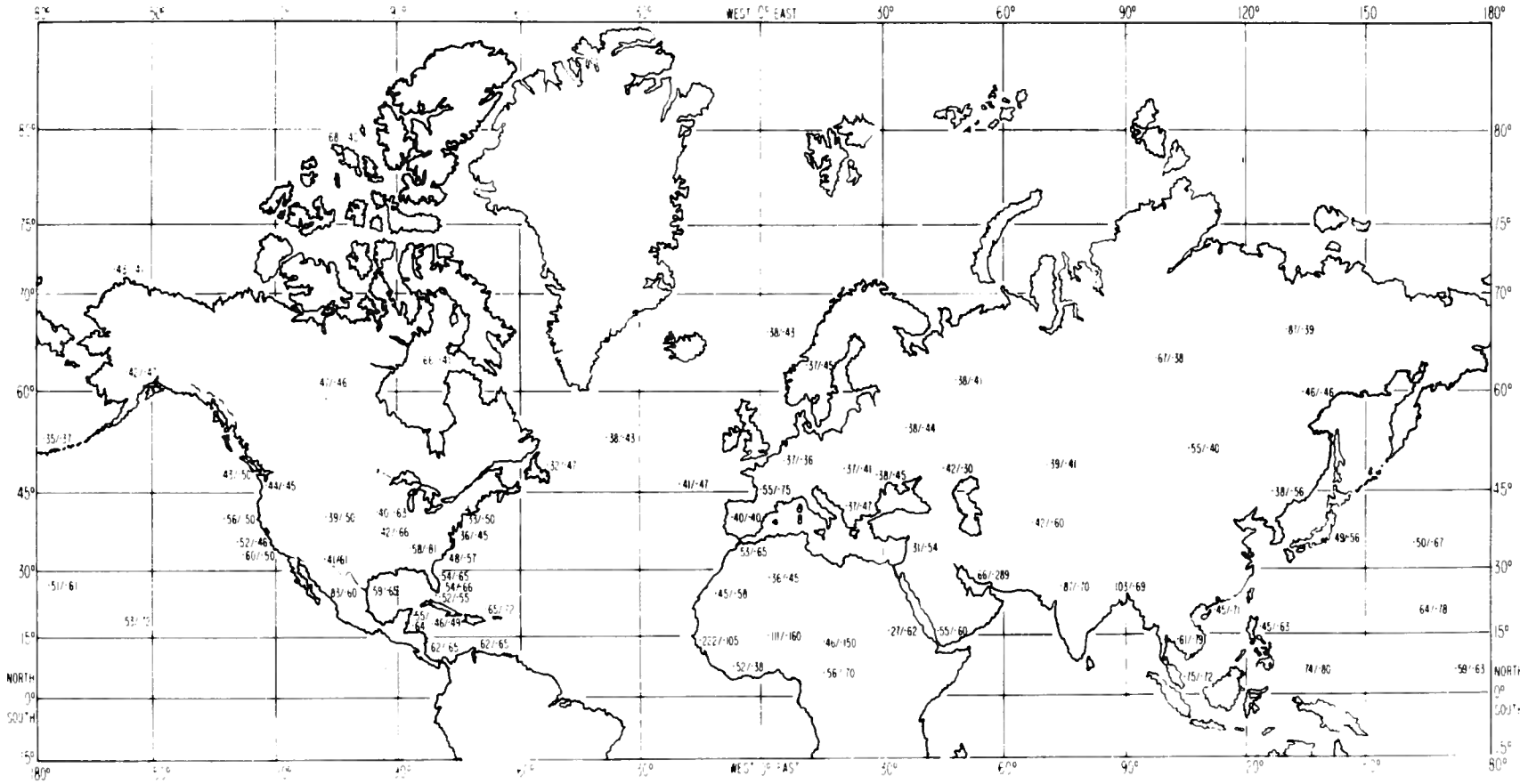

Figure 19. February and August median values of 100 m refractivity gradient [Samson, 1975].

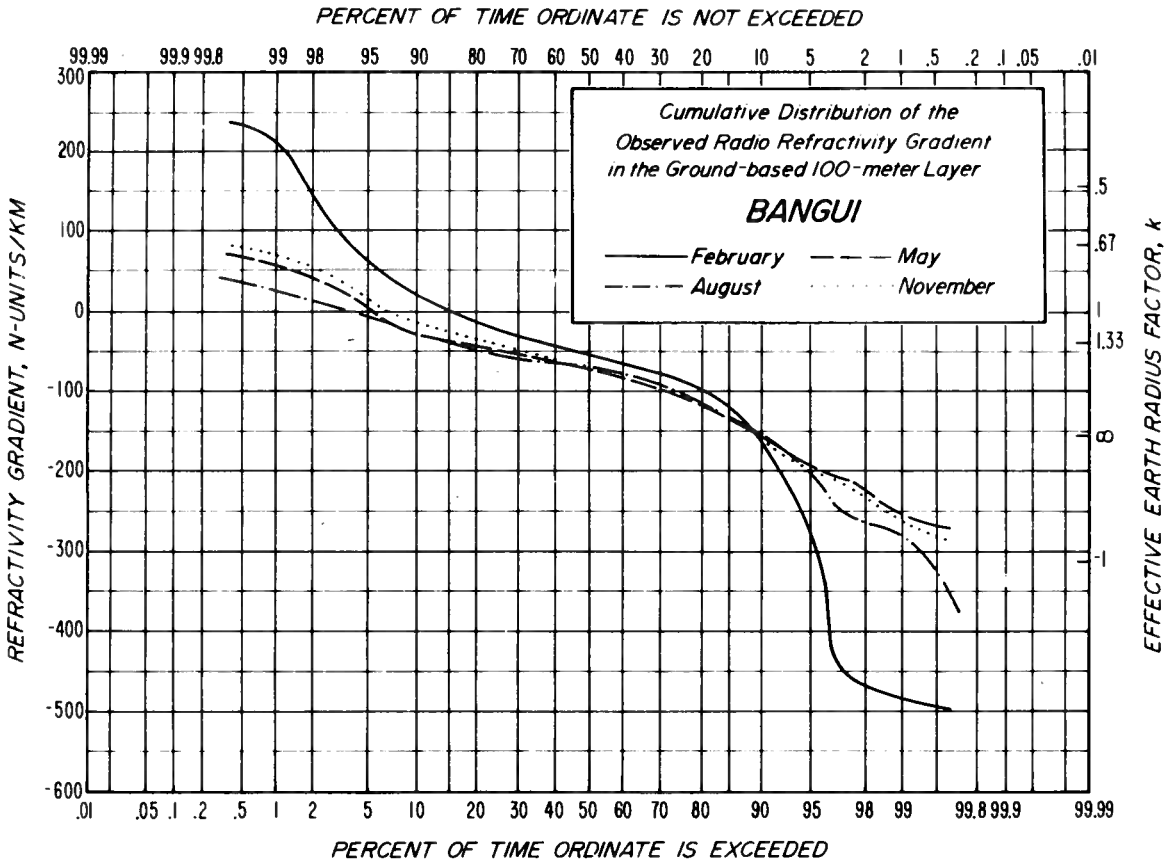

04°23'N, 18°34'E at 385 meters above MSL

Data: Radiosonde. 0300Z (0400 LST): 8/52 - 2/53
0400Z (1500 LST): 5/53 - 11/55
0500Z (0600 LST): 2/56 - 11/59
0600Z (0700 LST): 2/60 - 8/60
Note: Last 3 periods observations only every other day.

Temperature (°F): January 91/67; July 86/69

Mean Dewpoint (°F): January 69; July 73

Precipitation (inches): Annual 61.4; August 8.86; January 0.83

Located on the Ubangi River; a wooded, hilly area but some marshy areas in vicinity. A hot and humid monsoon climate with June-October rainy season in southwest monsoon and the dry season October-March in the northeast trade winds.

Figure 20. Observed gradients at Bangui, Central African Republic [from Samson, 1975].

4. THE ANOMALOUS FIELDS

The quantitative determination of the anomalous radio field behavior (for an expected refractivity structure near the surface) is based upon the applicable electromagnetic theory, sometimes referred to as duct-propagation theory. This consists of several theoretical methods [Kerr, 1951; Fock et al., 1958; Brekhovskikh, 1960; Budden, 1962; Wait, 1962; Fock, 1965; Rotheram, 1973 and 1974]. These may be considered as extensions of two basic formulations of propagation theory, the Booker and Walkinshaw [1946] mode theory and the Furry [1946] asymptotic theory; i.e., extensions for a wide variety of mathematical approximations to the refractivity structure within the duct.

Many experimental, studies -- ranging from the Canterbury Project [Unwin, 1951] to those of Jeske and Brocks (1966), Pidgeon [1970], and Wickerts [1970] -- have been undertaken to provide experimental verification of this guided mode of duct propagation. The verification to date has been impressive, but largely qualitative. That is, the salient features of the theory have been demonstrated, but full quantitative agreement is largely lacking. Although this undoubtably reflects the difficulty of adequately monitoring refractivity structures during the experimental studies, it also indicates some inadequacy of the theory. That is, departures of the (sea-surface or elevated) refractivity layers from a simple model (a refractivity profile of fixed vertical extent that is horizontally uniform) can eliminate some modes anticipated by present theory and also introduce additional unanticipated modes and mechanisms of propagation. For example, the theory is most suitable for evaluating propagation between two terminals well immersed within a continuous duct [Wait and Spies, 1969; Fruchtenicht, 1973] or between one terminal immersed in the duct and propagation via leakage from the duct to the other terminal just

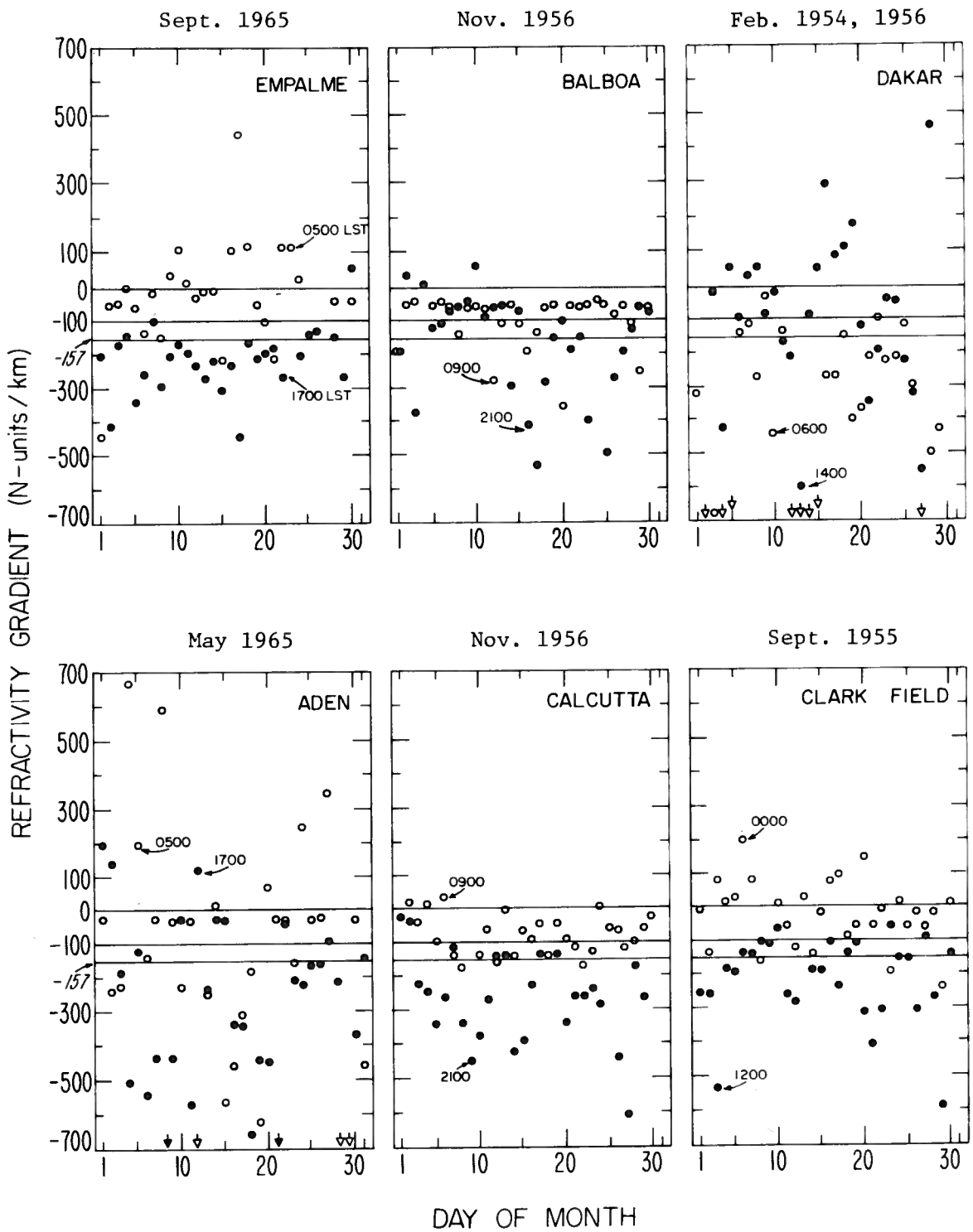

Figure 21. Diurnal variability in surface refractivity gradients.

exterior to (above or below) the duct [Chang, 1971; Ratner, 1976]. However, the applications of most pressing interest are for propagation via a (surface or elevated) duct when one or both terminals are exterior to the duct; the corresponding observational data substantiates received fields stronger than could be accounted for by the duct leakage determined from present theory. Of course, the theory assumes a duct that is horizontally uniform.

The mode-matching technique of Bahar and Wait [1965] and Bahar [1968, 1974] should permit extension of the theory so as to yield estimates of the attenuation and leakage attributable to variation (along the duct) of the refractivity gradient and its vertical extent. In addition, further extensive numerical evaluation of the asymptotic theory by computer or alternate formulations [Rulf 1968; Morawetz and Ludwig, 1968; Dougherty 1969] would aid the prediction and application problem. Application of the theory, and their expected extensions, to the prediction of anomalous fields on an operational basis requires their reduction to engineering-type curves or formulas.

4.1 Duct Geometry

The theoretical developments and the observational data outlined above appear sufficient to approximate the ducting phenomenon for radio regulation purposes. In that application, the concern is estimating the liklihood of inter-system interference. For example, in system design, wherein one must achieve a desired performance, the design engineer anticipates standard propagation, but must guard against those unusual conditions for which anomalous propagation would degrade the received signal. The design engineer seeks to achieve, for his communications system, a received signal (and performance) that exceeds a specified level almost all (99%, 99.9%, etc.)

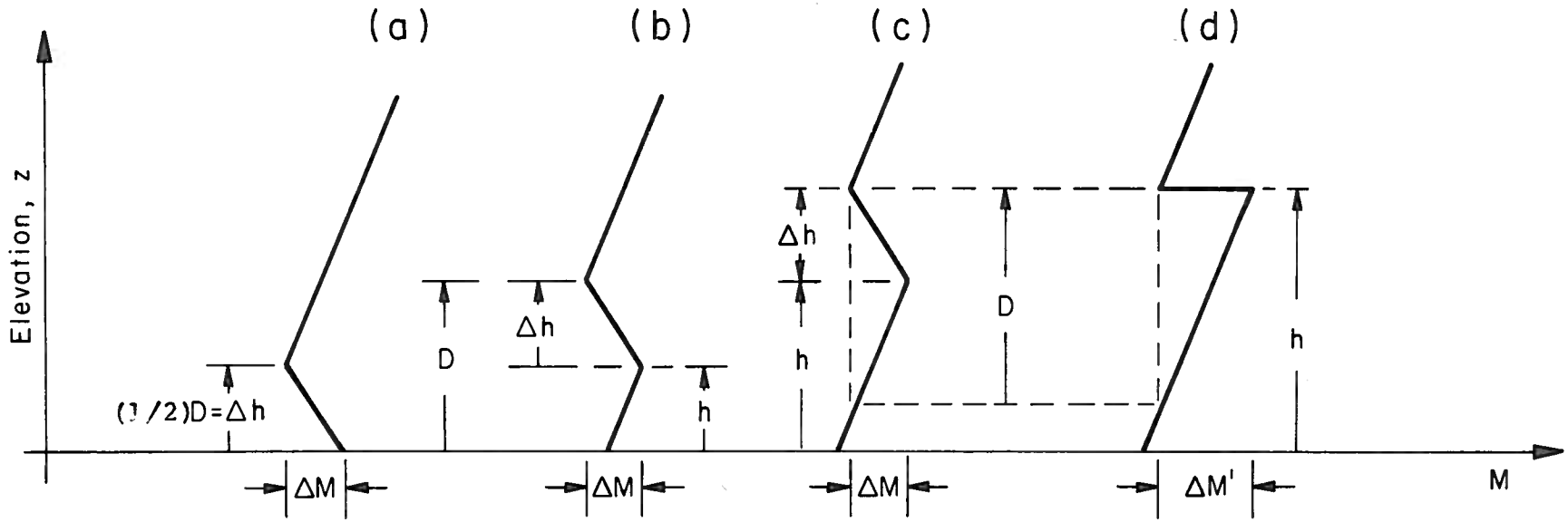

(a) Ground-based layer, Ground-based duct

(b) Elevated layer, Ground-based duct

(c) Elevated layer, Elevated duct

(d) Elevated layer and duct approximated with an M-discontinuity.

Figure 22. Elevated-layer and surface-layer parameters for ducting conditions.

77 x 0654

of the time -- one could day he requires a pessimistic (lower-bound) estimate of the field. However, if the system design is to be acceptable to the regulatory authority, the design engineer must also guard against those unusual conditions for which anomalous propagation would enhance reception of the signal by another system. The design engineer seeks to limit the received signal so as to exceed a specified level for as little (1%, 0.1%, etc.) a time as possible -- he requires an upper-bound estimate of the field. The present state of ducting theory and observational data does permit estimates of the upper bounds of ducted fields.

Let us consider a simplified geometry of the propagation ducts, as in figure 22. There, the refractive index structure n(h) has been approximated (in terms of its modified refractivity structure M(h) by a piecewise-linear structure [Furry, 1946; Kerr, 1951; Wait, 1962 and 1970; Andrianov, 1975; Ratner, 1976]. The modified index of refraction m is defined from Snell's Law for a spherically stratified earth's atmosphere as [Chap. 3, Bean and Dutton, 1968]

$$m = n\ (1 + \frac{h}{r_o}) \approx 1.0 \quad . \tag{3a}$$

Here, r_o is the earth's radius of approximately 6370 km. The refractive index n is related to the refractivity N by

$$n = 1 + N\ 10^{-6} \approx 1.0 \quad . \tag{3b}$$

Similarly,

$$m = 1 + M\ 10^{-6} \approx 1.0 \quad , \tag{3c}$$

so that

$$M \approx N + 157h \tag{3d}$$

in M units. Similarly, its gradient (in M units/km) is related

to the refractivity gradient (in N units/km) by

$$\frac{\Delta M}{\Delta h} = \frac{\Delta N}{\Delta h} + 157 = \frac{\Delta m}{\Delta h} \cdot 10^6 \quad . \tag{4}$$

Since the critical refractivity gradient (for trapping) is nominally -157 N units/km (Chap. 4, Bean and Dutton, 1968), the corresponding critical modified refractivity gradient is 0.0 M units/km. In figure 22, the gradients just above and below the superrefractive layer ($\Delta M/\Delta h \leq 0.0$) represent gradients of the order of 117.75 M units/km, corresponding to the "4/3 earth" gradient of -39.25 N units/km. The gradient below the layer could also, of course, be subrefractive ($\Delta M/\Delta h > 157$ M units/km).

Figure 22 depicts four ducts; (a) and (b) are ground-based, (c) and (d) are elevated. In (b), (c), and (d), the superrefractive layers ($\Delta M/\Delta h \leq 0.0$) are all elevated. Note that the ground-based ducts (a) and (b) involve a lower boundary determined by the ground. The elevated duct's lower boundary is defined by the gradient just below the layer; i.e., both the superrefractive layer and the one below it have the lapse rate ΔM in common within the duct. The duct width or thickness D is given for figures 22(a) and (b) by

$$D = 2\Delta h \quad , \quad h=0 \tag{5a}$$

and

$$D = \Delta h + h \ , \quad 0 \leq h \leq |\Delta M|/G \quad , \tag{5b}$$

respectively. Otherwise

$$D = \Delta h + |\Delta M|/G, \quad h > |\Delta M|/G \quad , \tag{5c}$$

for figures 22(c) and 22(d), where the superrefractive layer has the gradient $\Delta M/\Delta h < 0.0$ and the underlying gradient is indicated by G (>0.0 M units/km). For the commonly assumed refractivity gradient of -39.25 N units/km, the modified refractivity gradient G would be 117.75 M units/km. Then,

each of these ducts may be approximated by one with a discontinuous M profile; the elevated duct (c) is approximated by the equivalent duct (d). The M-discontinuity $\Delta M'$ is related to the actual M-lapse ΔM by

$$\Delta M' = G\ D \quad . \tag{6}$$

For the duct (a), therefore, $\Delta M' = 2\Delta M$. The advantage of introducing the modified refractive index is to transform a spherically stratified refractivity structure above a spherical earth into planar layers above a flat earth. Of course, the corresponding rays then become straight lines for a modified refractivity gradient of zero. However, for negative gradients, they have a curvature whose center is below the earth's surface and the emitter; for positive gradients they have a curvature whose center is well above the surface and emitter [Furry, 1946; Ikegami, 1959].

Figure 23 provides a crude representation of elevated duct propagation. There, we have employed ray-theory to illustrate the situation for a linear modified-refractivity profile. For a signal source at A in the elevated duct, the wave launched at, or exceeding, the critical angle ($|\theta| \geq |\theta_c|$) can propagate to points outside the duct (such as E', C', and C"). Waves launched at an angle $|\theta| \leq |\theta_c|$ are trapped; they propagate (via D, D', or D") to points within the duct (such as P or Q). The critical trapping angle is given, in milliradians, by [Gough, 1962]

$$\theta_c = \sqrt{2|\Delta M|} \quad , \tag{7}$$

for ΔM in M units. The trapped waves leak energy from the top of the duct (such as at D' to C' and E to P').

Radio waves launched from outside the duct and incident on the duct at a zero grazing angle can be trapped (such as from A' to E to P); otherwise, they traverse the duct (such

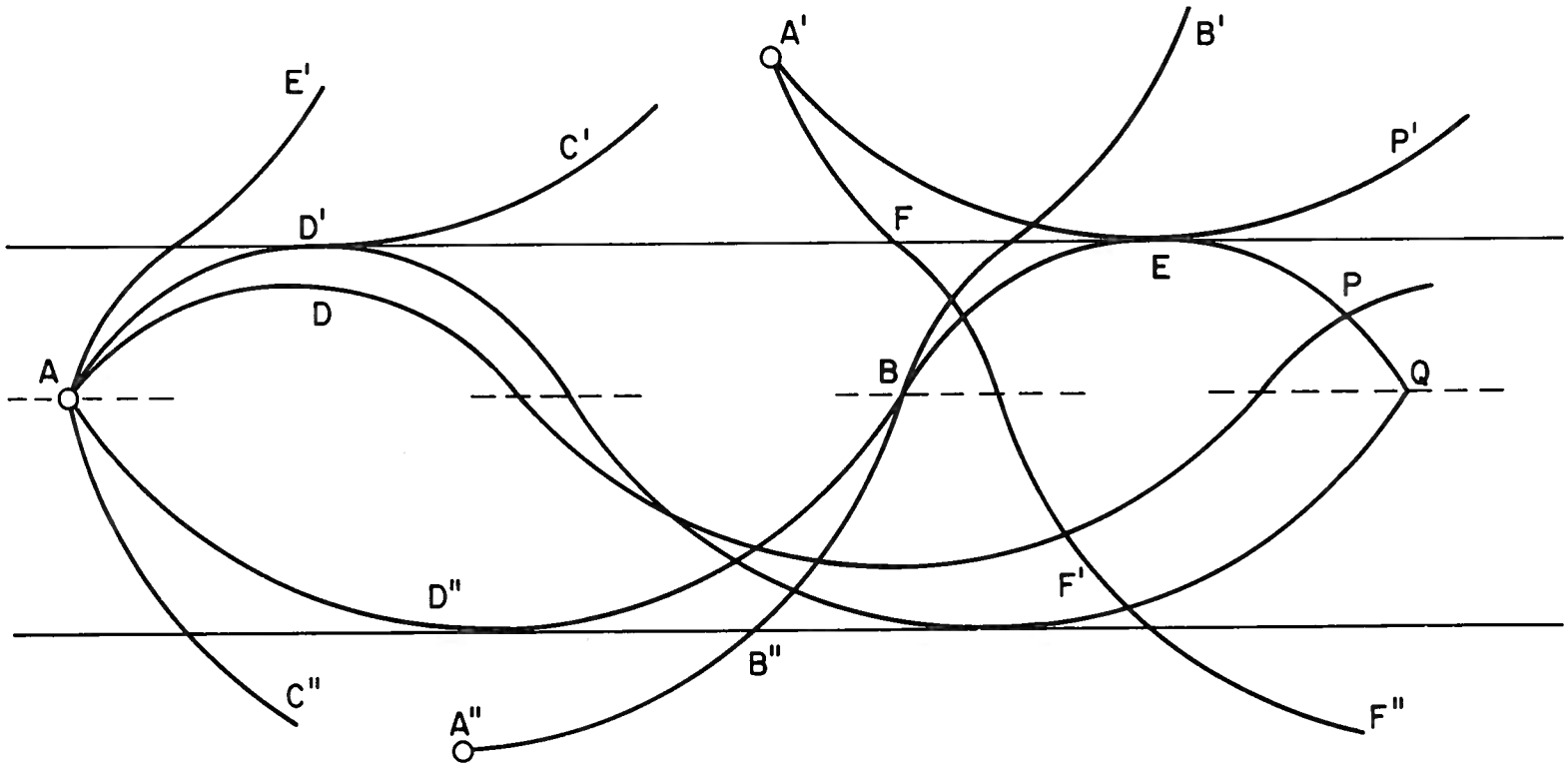

Figure 23. Ray-theory representations of elevated-duct propagation.

77X 0655

as from A' to F to F' and F"). If F' or F" is a point on the ground, the wave will be reflected to again traverse the duct to the region above the duct. For trapping to occur, elementary theory gives a minimum frequency of

$$f_{min} \approx \frac{240}{D\sqrt{|\Delta M|}} \tag{8}$$

in gigahertz, where the modified refractivity lapse M is in M units and the duct thickness D is in meters [Kerr, Chap. 1, 1951; Skillman, 1969].

Ray theory also implies that a wave originating exterior to and below the duct (where $\Delta M/\Delta h>0.0$) cannot be trapped within the duct. For example, a ray launched from A" below the duct will pierce the duct at B", pass B at an angle exceeding $|\theta_c|$, and traverse the duct and its upper boundary to B'. Since there can be no trapping of a ray from A", by reciprocity, there can be no leakage of trapped waves to points below the duct. This is misleading, of course. The full wave solutions evaluated by Chang [1971] and Ratner [1976] quantify the leakage both above and below the duct; by reciprocity, radio waves can be trapped within the duct from emitters external to the duct.

4.2 Approximations For Interference Estimates

In his text, Wait [1962] treated the problem of duct propagation extensively, placing the wide variety of solutions and applications into a common context. Since then, the full-wave solution for propagation through an atmospheric duct has been more fully evaluated for the (piecewise) linear variation of refractivity within, and in the vicinity of, the duct.

For a signal source and observer both well immersed in a duct, Wait [1969] showed that the signal is propagated along the duct by modes with very low propagation losses. For example, for standard atmospheric conditions ($\approx$4/3 earth or $\Delta M/\Delta h\approx 117$ M units/km) above and below an M-discontinuity

(figure 22d), Wait determined losses of $\alpha \leq 0.1$ dB/km for the first four (earth-detached) modes of propagation [Wait, 1969]. Further, Ratner [1976] showed that for frequencies greater than a critical value,

$$f_c = \frac{1572}{D^{1.8}} \text{ GHz} \tag{9}$$

(where D is the duct thickness in meters), the same full-wave solution will determine the first-mode attenuation coefficient as $\alpha \leq 3$ dB/(100km). The corresponding basic transmission loss (in decibels) is

$$L_{bD1} = 92.45 + 20\log f + 10\log r + 0.03\, r, \tag{10}$$

where f is the transmission frequency in gigahertz and r is the range in kilometers. This loss is considerably less than the free space value, for which $\alpha=0$ and the coefficient of the third term of (10a) is doubled. To these authors' knowledge, Johnson [1965] was the first to report air-to-air observational data that exhibited this r^{-1} received-signal-power variation with range, although it is suggested by some of Ringwalt and Macdonald's data [1961].

Wait [1969] and Ratner [1976] have shown that, when the M-discontinuity is replaced by the more realistic super-refractive layer ($\Delta M/\Delta h<0.0$ M units/km) of finite depth $\Delta h>0$, both the attenuation coefficient α and the critical frequency f_c increase with Δh. Hence, the expressions presented above for the M-discontinuity duct provide convenient, lower-bound estimates of duct propagation loss.

As a practical matter, we must also consider the aperture/medium coupling loss. For example, the ray-theory representation of figure 23 suggests that only that portion of the energy

radiated at elevation angles $-\theta_c \le \theta \le \theta_c$ are trapped and propagated along a uniform duct. Therefore, for each antenna, we may approximate the coupling loss by

$$\begin{aligned} A_c &= 10\log(2|\theta_c|/\Omega) \ , \quad 2|\theta_c| < \Omega \ , \\ &= 0.0 \text{ dB} \qquad\qquad , \quad 2|\theta_c| \ge \Omega \ , \end{aligned} \tag{11}$$

for a half-power-point antenna beamwidth Ω.

When only one terminal is within the duct, an uncertainty arises as to the proper coupling loss (from exterior to interior of the duct, or vice versa). For example, in the case of a horizontally uniform duct with one terminal within the duct and the other terminal above the duct, Ratner [1976] has estimates of the leakage loss from the duct to the exterior terminal (or by reciprocity, of the coupling loss). However, for the non-uniform ducts commonly met in nature, the coupling loss in decibels may be less. For the exterior terminal below the duct, the leakage computed for the uniform duct [Chang, 1971; Ratner, 1976] is probably too low for the realistic non-uniform duct. For "end-fire" propagation into a duct, (11) may be suitable with $2|\theta_c|$ replaced by the ratio of the duct width to the distance from the duct end to the external terminal [Misme, 1960]. Observational data suggest that (for the one terminal in, one terminal out, situation) a reasonable upper-bound estimate of the ducting basic transmission loss would be

$$L_b = 92.45 + 20\log f + 20\log r \text{ dB}. \tag{12}$$

This is the free-space loss, where the frequency f is in gigahertz and the range r is in kilometers. That is, it is assumed that the duct propagation loss due to leakage along the duct, the antenna coupling loss (for the antenna immersed within the duct), and the interior/exterior coupling loss is sufficient

to change the variation of received signal power with range to an r^{-2} dependency at best. See Vergara et al., [1962] and Richter and Hitney [1975].

When both terminals are exterior to the duct, we are not concerned with antenna/media coupling losses such as (11), but we are concerned with two interior/exterior coupling losses where the path from each antenna intercepts the duct (such as in figure 1). Again, for both terminals above the duct, the full-wave solutions of leakage loss [Chang, 1971; Ratner, 1976] might be somewhat high for the more common, horizontally non-uniform ducts. For both terminals below the non-uniform duct, the full-wave solution is too pessimistic. Observations suggest that an lower-bound estimate (for one or both terminals above the duct) would be a free-space loss, such as (12). For both terminals below the duct, a lower-bound estimate would appear to be free-space plus 20 dB [Dougherty et al., 1970].

$$L_b = 112.45 + 20\log f + 20\log r \quad \text{dB}. \tag{13}$$

4.3 Occurrence

For the national or international regulatory agencies, the foregoing expressions -- (10), (11), (12), and (13) --- will permit a determination of basic transmission loss and, therefore, of the coordination distance. However, additional information is vital. What is their occurrence; i.e., how often will these losses apply, how will they vary with geographical location? The available experimental data permit only partial answers.

The essential requirement for a markedly enhanced field is the presence of a supercritical atmospheric layer ($\Delta N/\Delta h \leq -157$ N units/km or $\Delta M/\Delta h < 0.0$ M units/km). In the case of sea-surface ducts (that are formed from surface

evaporative layers or slightly elevated advective layers), Section 3 indicates that they are semi-permanent fixtures in subtropic and coastal waters, decreasing in prevalence in a poleward direction. The evaporative layers have been mapped over about half the ocean areas, although the deeper advective ducts have not been as extensively mapped over water. Of course, the initial gradients have been mapped in quantitative detail over land [Bean et al., 1966].

Beyond quantitative estimates of the occurrence of atmospheric layers and ducts, estimates of specific characteristics are also necessary. For example, application of (9) requires a knowledge of the spatial and temporal distributions of duct thicknesses beyond the facts that evaporative ducts typically extend from the surface up to about 15 m, whereas advective ducts typically extend to at least 25 m. Of course, either of these values will determine a typical critical frequency from (9) and also whether specific terminal heights would lie within or extend above the typical sea-surface (evaporative or advective) ducts. However, the vital associated information --- percent of the time --- is still lacking. Early efforts at prediction incorporated data on duct gradient and thickness into the approximate expression (8) for trapping frequency; this data was made available as charts of contours of percent occurrence of sea-surface ducts capable of trapping S, X, and D-band transmissions [Crozier et al., 1952; Cowan, 1953; Gossard 1957 and 1964; Gossard and Anderson, 1956a and 1956b; Bean et al., 1966]. These have not been improved upon or extended since, so that wider geographical coverage as well as data on duct-top heights (required to determine whether communication terminals are above or within a surface duct) are still lacking. One could apply (9) to the predicted occurrence of extended range for S, X, and K-band to determine the associated duct thicknesses as, respectively, 47, 24, and 16 m.

This result, the maps of percent occurrence, and equations (10) and (12) may then serve as the best available solution for portions of the world.

For elevated layers and ducts formed by advection or subsidence, Section 2 indicates that such layers range from semi-permanent conditions (in the tradewind and some coastal regions) to increasingly rare phenomena as we move poleward. Although there are considerable radiosonde data available as historical records and on a worldwide basis, only a very limited amount have been processed into the refractivity-height profiles from which layer characteristics can be determined. Mappings of some characteristics have been long available: very sketchily on a worldwide basis [Randall, 1964; Cahoon and Riggs 1964]; in more detail for localized areas [Hall, 1969]; and in appreciable detail for the Atlantic tradewind region [Dougherty et al., 1967]. All of such data could be greatly improved by further processing of data. For example, the Atlantic tradewind system is well behaved and adequately described in terms of temporal distributions of gradients, heights, thickness, etc. as the high-pressure cells follow a well-defined pattern of shifting with the season (between the West Indies and the Madeira Islands in the North Atlantic and near Ascension Island in the South Atlantic). The resulting elevated ducts have a thickness of the order of 100 to 250 m so that (9) indicates a critical frequency of about 76 to 395 MHz. Of course trapping requires gradients less than -157 N units/km, which are not always achieved by the tradewind inversion layer; for example trapping gradients occur for about 2/3 times the occurrences indicated in figure 3. Therefore, the occurrence of tradewind trapping layers (ducts) in the Atlantic tradewind regions varies with the season from about 30 to 55%. Similarly, these elevated ducts increase in height from east to west and range with the season from about 1.2 to 3.0 km above

the sea-surface. The appropriate transmission loss for terrestrial systems is given by (13). For one or both communication terminals airborne, (11), or (12) is appropriate. It is useful to note that the base of the tradewind inversion (ducting) layer tends to coincide with the cloudtops; protrusions of clouds above the general cloudtop level are one indication of the localized weakening or disruption of the inversion layer.

5. CONCLUSION

Since 1944, some prediction charts have been available for estimating the occurrence and characteristics of the superrefractive elevated layers or surface layers that constitute surface ducts. The world's land surface and most of the waters bordering the Asian continent have been so charted for both advection and evaporation layers. Most of the world's oceans have been so charted for the occurrence of surface advection layers and also for a few of their characteristics pertinent to anomalous propagation. These charts have limitations due to the available marine meteorological data. The data are particularly inadequate in space and temporal coverage. For example, much more data would be useful for the temporal and spatial variation of the layer (or duct) vertical thickness and horizontal extent. Programs such as the BOMEX Sea-Air Interaction Study and the U.S. Coast Guard National Data Buoy Project could lead to a substantially improved data base for the prediction of sea-surface duct characteristics.

Since 1958, estimates have become increasingly available for the occurrence of elevated layers that are sufficiently superrefractive to serve as the upper portion of elevated atmospheric ducts. Summary data on the characteristics of these elevated layers are most sparse overland; the tradewind-regions of the world appear to yield the most systematic characteristics, although there is presently much less data available

for the Pacific than for the Atlantic tradewind regions. The available meteorological (radiosonde) data has yet to be adequately exploited and processed; one could then determine elevated layer characteristics on a more satisfactory world-wide basis.

In addition to the referenced data, further information is available from the referenced authors, particularly from Fedi of Italy, Hall of the United Kingdom, Ikegami of Japan, Jeske of West Germany, Misme of France, Richter of the U.S., and Wickerts of Sweden.

From the point of view of operational system design (for communications or long-distance monitoring via ducts), there is also a further limitation. For example, the applicable propagation theory is well advanced; their extensions presently under investigation are very likely to encompass the departures of observed ducts from the horizontally uniform model. The limitation results primarily from the fact that the available solutions have not been reduced as yet to the engineering-type formulas or curves required for the prediction of these anomalous fields on an operational basis.

From the point of view of radio regulation and estimating interference, however, the observational data and the theory already permit lower-bound predictions of transmission loss. For frequencies at or above that given by (9), the transmission loss between terminals immersed in the duct is given by (10) and (11); this can be a gain relative to free-space. For one terminal immersed in the duct and one terminal external to the duct, the basic transmission loss is given by (12). For both terminals external to the duct and one or both above the duct the lower-bound estimate is free space given by (12). If both terminals are below the duct, the lower-bound estimate of the basic transmission loss is free space plus 20 dB given by (13). However, prediction of the associated percent occurrence is presently hampered by inadequate summaries of elevated duct characteristics.

6. REFERENCES

Ament, W. S. (1959), Airborne Radiometeorological Research, Proc. IRE 47, No. 5, May, 756-761.

Ament, W. S., W. Binnian, W. W. Carter, M. Katsin, and D. T. Olmsted (1962), Microwave propagation measurements over the Pacific Ocean, U. S. Naval Research Lab. Report 5687, February.

Anderson, L. J., and E. E. Gossard (1952), Extended coverage prediction of microwave fleet radars, Navy Electronics Laboratory Report 302, (8 May 1952) San Diego, California.

Anderson, L. J., and E. E. Gossard (1955), Prediction of oceanic duct propagation from climatological data, Trans. IRE AP-3, October, 163-167.

Andrianov, V. A. (1975), Mechanisms of tropospheric microwave propagation for a linear segmented profile of the refractive index, IEEE Trans. AP-23, No. 5, September, 602-607.

Arrola, W. A. (1957), Refractive index profiles and associated synoptic patterns, Bul. American Meteorol. Soc. 38, No. 4. 212-220.

Bahar, E. (1968), Scattering of VLF radio waves in the curved earth-ionosphere waveguide, Radio Sci. 3, (2), 145-154.

Bahar, E. (1974), Propagation in ducts and waveguides possessing irregular features - full wave solutions, AGARD Conference Proceedings No. 144 on EM Wave Propagation Involving Irregular Surfaces and Inhomogeneous Media NATO, The Hauge, March, 7-1 to 7-12.

Bahar, E., and J. R. Wait (1965), Propagation in a model terrestrial waveguide of nonuniform height: theory and experiment, J. Res. NBS 69D, 1445-1463.

Bean, B. R., B. A. Cahoon, C. A. Samson, and G. D. Thayer (1966), A World Atlas of Atmospheric Radio Refractivity, ESSA Monograph No. 1, Natl. Tech. Information Service (NTIS Access No. AD648-805).

Bean, B. R., and E. J. Dutton (1968), Radio Meteorology, Dover Publications, Inc., New York.

Beckmann, P., and A. Spizzichino (1963), The scattering of Radio Waves by Irregular Surfaces, (Pergamon Press, N.Y.).

Booker, H. G. (1946), Elements of radio meteorology: How weather and climate cause unorthodox radar vision beyond the geometrical horizon, Proc. IEE Pt. 3A(1) 93, 69-78.

Booker, H. G., and W. Walkinshaw (1946), The mode theory of tropospheric refraction and its relation to wave-guides and diffraction, Meteorological Factors In Radio-Wave Propagation, The Physical Society, London.

Brekhovskikh, L. M. (1960), Waves in layered media, Academic Press, London.

Budden, K. G. (1962), The waveguide mode theory of wave propagation, Prentice-Hall, New York.

Cahoon, B. A., and L. P. Riggs (1964), Climatology of elevated superrefractive layers arising from atmospheric subsidence, World Conference of Radio Meteorology, Boulder, Colorado (American Met. Soc., Boston, Mass.).

Chang, H. T. (1971), The effect of tropospheric layer structures on long-range VHF radio propagation, IEEE Trans. AP-19, No. 6, November, 751-756.

Cowan, L. W. (1953), Forecasting refractive index profiles in the atmosphere, Tech. Paper No. 2, U.S.A.F. 3rd Weather Group, Ent Air Force Base, Colorado Springs, Colo.

CCIR (1974a), Radio meteorological data, Report 563, Volume V Propagation In Non-Ionized Media, 96-112, CCIR XIIIth. Plenary Assembly, Geneva (NTIS Access No. PB244005).

CCIR (1974b), Evaluation of propagation factors in interference problems at frequencies greater than about 0.6 GHz, Report 569, Volume V, Propagation In Non-Ionized Media, 258-287, CCIR XIIIth Plenary Assembly, Geneva (NTIS Access No. PB244005).

CCIR (1974c), Reports 344-2, 573, and 259-3 of Volume VI, Ionospheric Propagation, CCIR XIIIth Plenary Assembly, Geneva (NTIS Access No. PB244006).

Crozier, A. L., F. Pogar, G. Yee, S. Porter, E. E. Gossard, J. Hill, L. J. Anderson, and G. T. Dampier (1952), Far East radio-radar propagation conditions for fleet units, Navy Electronics Laboratory Report 319, San Diego, Calif.

Day, J. P., and Trolese, L. G. (1950), Propagation of short waves over desert terrain, Proc. IRE, 38, No. 2, 165-175.

Dougherty, H. T. (1964), Bibliography of fading on microwave line of sight tropospheric propagation paths and associated subjects, NBS Tech. Note No. 302 (U. S. Government Superintendent of Documents, Washington, D. C.).

Dougherty, H. T. (1968), A survey of microwave fading mechanisms, remedies and applications, ESSA Tech. Rept. ERL69-WPL 4, Natl. Tech. Information Service (NTIS Access No. COM-71-50288).

Dougherty, H. T. (1969), An approximate closed-form method of solution for the diffraction of radio waves by irregular surfaces, Dissertation Abstracts, B, 294, Engineering, 3742-B. See also Radio Science 5, No. 1, January, 1970.

Dougherty, H. T., L. P. Riggs, W. B. Sweezy (1967), Characteristics of The Atlantic trade wind system significant for radio propagation, (NTIS Access No. AD 651541).

Dougherty, H. T., R. E. McGavin, and R. W. Krinks (1970), An experimental study of the atmospheric conditions conducive to high radio fields, Office of Telecommunications, OT/ITS Report 4 (NTIS Access No. COM-75-11138/AS).

duCastel, F., P. Misme, and J. Voge (1960), Sur le role des phenomenes de reflexion dans la propagation lointaine des ondes ultracourtes, Electromagnetic Wave Propagation 670-683, Academic Press (New York).

Fedi, F. (1973), Introductory survey of Session IV, AGARD Conference Proceedings No. 127, NATO, Propagation Effects On Frequency Sharing, Rome, Italy.

Fleagle, R. G. (1970), Summary of the symposium on "Early Results from Bomex," Bull. Amer. Meteor. Soc. 51, (4), 319-320.

Fock, V. A. (1965), Electromagnetic diffraction and propagation problems, Pergamon Press, New York.

Fock, V. A., L. A. Wainstein, and M. M. E. Belkina (1958), Radiowave propagation in surface tropospheric ducts, Radio-tekhnika i elektronida 3, (12), 1400-1429.

Fruchtenicht, H. W. (1973), Characteristics and applications of line-of-sight duct propagation, NATO Adv. Study Inst. on Modern Topics In Wave Propagation Above 10 GHz, Especially Those Associated with Air-Sea Interaction, June, Sorrento, Italy.

Furry, W. H. (1946), Methods of calculating characteristic values for bilinear M-curves, Radiation Lab Report No. 795, February.

Gentilli, J. (1958), A Geography of Climate, The University of Western Australia Press, Perth, Australia.

Gerks, I. H. (1971), Computing the effects of tropospheric refraction at frequencies below 10 megahertz, Radio Science 6, No. 7, July 681-688.

Gossard, E. E. (1957), Air-sea refractive index difference charts for the Mediterranean-Southeast Asia areas, Bull. Amer. Meteor. Soc. 38 (5), 274-278.

Gossard, E. E. (1964), Radio refraction by the marine layer and its effect on microwave propagation, Research Report 1240, U. S. Navy Electronics Lab., San Diego, Calif.

Gossard, E. E., and L. J. Anderson (1956a), Near East and Southeast Asia radio-radar propagation conditions for fleet units, Navy Electronics Laboratory Report 683, San Diego, California.

Gossard, E. E., and L. J. Anderson (1956b), The effect of super-refractive layers on 50-5000 Mc non-optical fields, Trans. IRE AP-4, April, 175-178.

Gough, M. W. (1962), Propagation influences in microwave link operation, British IRE, 24, 53-72.

Guinard, N. W., J. Ransone, D. Randall, C. Purves, and P. Watkins (1964), Propagation through an elevated duct: Tradewinds III, Trans. IEEE AP-12, No. 4, July, 479-490.

Hall, M. P. M. (1968a), VHF radio propagation by doublehop reflection from a tropospheric layer, Proc. IEE, 115, No. 4, 503-506.

Hall, M. P. M. (1968b), Further evidence of VHF propagation by successive reflections from an elevated layer in the troposphere, Proc. IEE, 115, No. 11, 1595-1596.

Hall, M. P. M. (1969), Statistics of tropospheric radio-refractive-index soundings taken over a 3-year period in the United Kingdom, Proc. IEE 116, No. 5, May, 685-690.

Hall, M. P. M., and C. M. Comer (1969), Statistics of tropospheric radio-refractive-index soundings taken over a 3-year period in the United Kingom, Proc. IEE 116, No. 5, May, 685-690.

Hart, B. A., G. D. Thayer, and H. T. Dougherty (1971), Local and Diurnal Variations in Ground-Based Radio Refractivity Gradients at Tropical Locations, Office of Telecommunications Rept. OT/TRER 23 (NTIS Access No. COM-75-10831/AS).

Hirao, K., Y. Vesugi, and K. Tao (1952), Propagation characteristics of VHF over a distance of 125 km, J. Geomag. Geoelect. 4, 131-140.

Holden, D. B., E. F. Gossard, and R. U. F. Hopkins (1960), Radio meteorology and climatology of the Eastern North Pacific, Research Report 966, U. S. Navy Electronics Lab., San Diego, California.

Ikegami, F. (1959), Influence of an atmospheric duct on Microwave fading, IRE Trans. AP-7, No. 3, July, 252-257.

Ikegami, F. (1964), Radiometeorological effects in propagation over the sea and islands, Review of the Electrical Communication Laboratory, 12, Nos. 5-6, May-June, 312-324.

Jeske, H. (1964), Propagation of electromagnetic waves in the cm ato m bands over the ocean with special consideration of the meteorological conditions in the maritime boundary layer (in German), Hamburger Geophysikalische Einzelschriften, DeGruyter, Hamburg.

Jeske, H., and K. Brocks (1966), Comparison of experiments on duct propagation above the sea with the mode theory of Booker and Walkinshaw, Radio Science, Vol. 1, (new series) No. 8, 891-895.

Johnson, A. L. (1965), Airborne microwave communication test, AF-WP-O-Jan 65100, Systems Engineering Group, Wright-Patterson AFB, Ohio.

Katzin, M., R. W. Buchanan, and W. Binnian (1947), 3 and 9 centimeter propagation in low ocean ducts, Proc. IRE 35, No. 9. September 891-905.

Kerr, D. E. (1951), Propagation of short radio waves, Radiation Laboratory Series, Vol. 13, McGraw-Hill Book Co., Inc., New York.

Lane, J. A., and P. W. Sollum (1965), VHF transmission over distances of 140 and 300 km, Proc. IEE 112, No. 2, February, 254-258.

Lane, J. A., and I. E. Owolabi (1969), Anomalous propagation on VHF radio links in the United Kingdom, Electronic Letters 5, No. 26, December 27.

Misme, P. (1960), Le gradient equivalent mesure directe et calcul theorique, Annales Des Telecommunications 15, No. 3-4, 92-99.

Misme, P. (1973), Role des conduits atmospheriques dans les phenomenes de brouillage a grand distance, AGARD, Propagation Effects on Frequency Sharing, NATO, Conference Proceedings No. 127, Rome.

Misme, P. (1974), Affaiblissement de transmission en propagation guide par conduit atmospherique, Ann. des Telecomm. 29, No. 3-4, March-April, 1/10-10/10.

Miyake, M., and M. Donelan (1970), Airborne measurement of turbulent fluxes, J. Geophys. Res. 75, (24), 4506-4518.

Morawetz, C. S., and D. Ludwig (1968), An inequality for the reduced wave operator and the justification of geometrical optics, Comm. on Pure and Appl. Math. XXI, 187-203.

Murray, O. M. (1972), Long-Range VHF Survey In The Arabian Gulf, Marconi Technical Report MTR 72/34, March.

Noonkester, V. R., and H. V. Hitney (1974), Synoptic prediction of meteorological factors affecting tropospheric radio propagation, Naval Electronics Laboratory Center Tech. Report 1934, October.

Owolabi, I. E., and J. A. Lane (1973), Transhorizon propagation on v.h.f. radio links in the United Kingdom, Proc. IEE 120, No. 2, February, 165-172.

Paltridge, G. W. (1970), Reflection from elevated layers in the troposphere, Proc. IEE 117, No. 1, January, 23-26.

Pidgeon, V. W. (1970), Frequency dependence of radar ducting, Radio Sci., 5, (3), 541-550.

Randall, D. L. (1964), A summary of tropospheric duct meteorology at VHF and UHF as observed on a trip around the world. Feb. 8 to Mar. 15, 1963, World Conference On Radio Meteorology, Boulder, Colorado (American Met. Soc., Boston, Mass.).

Ratner, A. S. (1976), Propagation of Electromagnetic waves in elevated tropospheric ducts, to be published.

Richter, J. H., and H. V. Hitney (1975), The Effect of the Evaporation Duct On Microwave Propagation, NELC Report TR1949 April (San Diego).

Ringwalt, D. L., W. S. Ament, and F. C. MacDonald (1958), Measurements of 1250 Mc scatter propagation as function of meteorology, IRE Trans. AP-6, No. 2, 208-209.

Ringwalt, D. L., and F. C. MacDonald (1961), Elevated duct propagation in the tradewinds, IRE Trans. AP-9, No. 4, 377-383.

Rotheram. S. (1970), Ground-wave propagation at medium and low frequencies, Electronic Letters 6, No. 25, 794-795.

Rotheram, S. (1973), Theory of transhorizon propagation in the evaporation duct, Propagation of Radio Waves At Frequencies Above 10 GHz, London, U.K.; IEE Conference Publication No. 98, 70-75.

Rotheram, S. (1974), Scattering out of the evaporative duct, AGARD Conference Proceedings No. 144 on Electromagnetic Wave Propagation Involving Irregular Surfaces and Inhomogeneous Media, The Hague, Netherlands, March, pp 11-1 to 11-12.

Rulf, B. (1968), Uniform asymptotic theory of diffraction at an interface, Comm. on Pure and Appl. Math XXI, 67-76.

Samson, C. A. (1975), Refractivity gradients in the Northern Hemisphere, Office of Telecommunications Report 75-59, April (NTIS Access No. COM 75-10776/AS).

Saxton, J. A. (1951), The propagation of meteorological waves beyond the horizon, Proc. IEE, Pt. III 98, 360-369.

Schelkunoff, S. A. (1944), Microwave transmission in a non-homogeneous atmosphere, Bell Tel. Lab. Rep. MM-44-110-53.

Skillman, J. L. (1969), The effects of elevated tropospheric layers on radio wave propagation, Master's Thesis, E. E. Dept., University of Maryland, College Park, Md.

Sverdrup, H. U. (1943), Oceanography for Meteorologists, Prentice-Hall, Inc., New York.

Takahira, A., and H. Irie (1960), Characteristics of maritime advective duct and their effect on the micro wave propagation beyond the line of sight, Journ. Radio Res. Labs. 7, No. 33, September, 531-544, Tokyo, Japan.

Thayer, G. D. (1970), Radio Reflectivity of Tropospheric Layers, Radio Science, Vol. 5, No. 11, 1293-1300.

Unwin, R. S. (1951), Report of factual data from the Canterbury project, Vols. I-III, Dept. Sci. Ind. Research, Wellington, New Zealand.

USNEL (1952), Far-east radio-radar propagation conditions for fleet units, U.S. Navy Electronics Lab. Report 319, July.

USNWSC (1967), The analysis and forecasting of atmospheric radar refractivity, U.S. Naval Weather Service Command Report NAVAIR 50-1P-1.

Vergara, W. C., J. L. Levatich, and T. J. Carrol (1962), VHF air-ground propagation for beyond the horizon and tropospheric stability, IRE Trans. AP-10, No. 5, September, 608-621.

Wait, J. R. (1964), A note on the VHF reflection from a tropospheric layer, Radio Science 68D, No. 7, July, 847-848.

Wait, J. R. (1969), Reflection from subrefractive layers, Electronic Letters 5, No. 4, February 20, 64-65.

Wait, J. R. (1962), Electromagnetic Waves in Stratified Media, Chaps. XI and XII, Pergamon Press, New York. There is also a Second Edition, 1970.

Wait, J. R., and C. M. Jackson (1964), Influence of the refractive index profile in VHF reflection from a tropospheric layer, IEEE Trans. AP-12, No. 4, July, 512-513.

Wait, J. R., and K. P. Spies (1969), Internal guiding of microwaves by an elevated tropospheric layer, Radio Science 4, No. 4, 319-326.

White, R. F. (1968), Space diversity on line-of-sight microwave systems, IEEE Trans. COM-16, No. 1, February, 119-133.

Wickerts, S. (1970), The refractive index field in the lowest 2000 m of the atmosphere, FOA Reports 4, (3), 104 50 Stockholm 80, Sweden.

Yamada, R. (1961), Reflection of electromagnetic waves from a stratified inhomogeneity, IRE Trans. AP-9, No. 4, July, 364-370.

FORM OT-29
(3-73)

U.S. DEPARTMENT OF COMMERCE
OFFICE OF TELECOMMUNICATIONS

BIBLIOGRAPHIC DATA SHEET

	1. PUBLICATION OR REPORT NO.	2. Gov't Accession No.	3. Recipient's Accession No.
	OTR 76-107		

4. TITLE AND SUBTITLE
Anomalous Propagation and Interference Fields

5. Publication Date
December 1976

6. Performing Organization Code
OT/ITS

7. AUTHOR(S)
H. T. Dougherty and B. A. Hart

8. PERFORMING ORGANIZATION NAME AND ADDRESS
U.S. Department of Commerce
Office of Telecommunications
Institute for Telecommunication Sciences
Boulder, Colorado 80302

9. Project/Task/Work Unit No.
9107202

10. Contract/Grant No.

11. Sponsoring Organization Name and Address
Office of Telecommunications

12. Type of Report and Period Covered

13.

14. SUPPLEMENTARY NOTES

15. ABSTRACT *(A 200-word or less factual summary of most significant information. If document includes a significant bibliography or literature survey, mention it here.)*

This report presents some estimates of the enhanced fields deduced from the presently available theory and observational data. The fields of interest are the enhanced fields that are encountered in the presence of the stratified atmosphere, the ducting conditions associated with supercritical refractivity gradients both near the surface and aloft.

As a basis for estimating the likelihood of occurrence of these supportive conditions, the available information is surveyed. It is suggested that the access to computers and the availability of historical radiosonde data be exploited and the pertinent characteristics of elevated layers and their associated ducts be mapped on a worldwide basis to meet the interference prediction requirements of regulatory agencies.

16. Key Words *(Alphabetical order, separated by semicolons)*

17. AVAILABILITY STATEMENT

[X] UNLIMITED.

[ ] FOR OFFICIAL DISTRIBUTION.

18. Security Class *(This report)*
Unclassified

19. Security Class *(This page)*
Unclassified

20. Number of pages
69

21. Price:

☆U.S. Government Printing Office: 1976-777-948/75 Region 8